Effects of CDOM on clarity and phytoplankton in Lake Brunner.

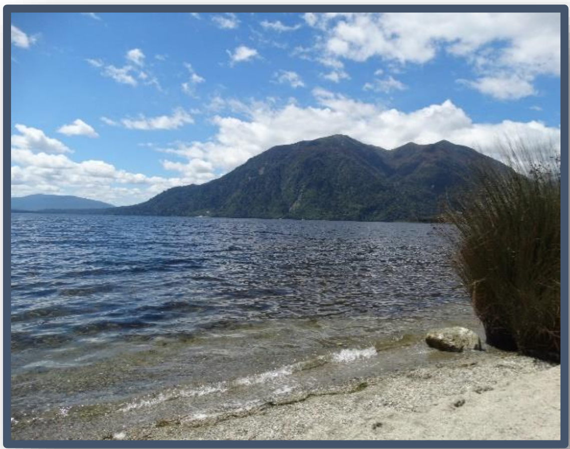

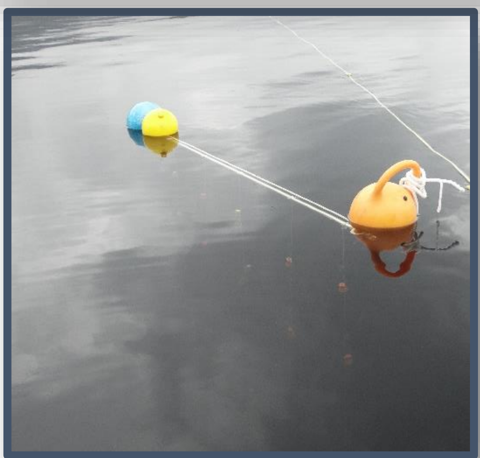

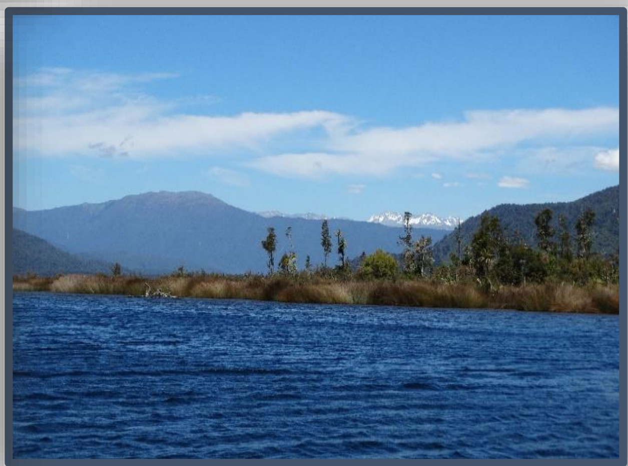

Author:

William Neefjes

Supervisors:

Piet Verburg (NIWA),
Rob Davies-Colley (NIWA),
Jeroen de Klein (WUR)

Date:

July 2015

Institutes:

National Institute for Water and Atmosphere Research (NIWA)

Wageningen University (WUR)

Place:

Hamilton, New Zealand

NIWA Taihoro Nukurangi

WAGENINGEN UR For quality of life

Abstract

Lake Brunner is an oligotrophic lake on the West Coast of the New Zealand's South Island that is somewhat stained by coloured dissolved organic matter (CDOM). Since 1992, Secchi depth has been decreasing at a time of increasing concentrations of chlorophyll *a*, which in turn appears to be a response to increased nutrient loading. Because CDOM can limit light penetration and may thereby inhibit phytoplankton growth, the effects of further nutrient enrichment on eutrophication might be diminished by CDOM loads from the catchment. This study examined interactions between CDOM and chlorophyll *a*, and their effects on visual clarity and light penetration in Lake Brunner. A mass balance on CDOM was constructed including inflows and outflows of CDOM to the lake, and losses by photochemical degradation of CDOM, which were determined experimentally.

The results showed that Secchi depth has increased again in recent years, and now is similar to that in 1992. Statistical analysis by multiple linear regressions showed that CDOM is the main attenuator of light penetration in the water column. However, CDOM and chlorophyll *a* are not correlated, suggesting that light attenuation by CDOM may not inhibit phytoplankton growth in Lake Brunner. Tributary inflows of CDOM into the lake were found experimentally to be higher than outflows, at least in summer months, suggesting that about 20% of the inflowing CDOM is lost. Experiments on photochemical degradation suggest that this loss mechanism is negligible, so another mechanism must be responsible for CDOM loss within the lake such as sorption to terrigeneous solids settling to the lake bottom. Lastly, there could be the possibility that CDOM input varies seasonally and is higher in summer. This would be consistent with higher concentrations of epilimnetic CDOM than hypolimnetic CDOM (= seasonally isolated winter water) in Lake Brunner during summer months.

Acknowledgments

I would like to thank the National Institute for Water and Atmosphere Research (NIWA) for facilitating and funding part of my research. I would like to thank Piet Verburg and Rob Davies-Colley for the supervision and help on my thesis. Furthermore, I would like to thank the West Coast Regional Council (WCRC) for funding my research, and helping out with the logistics of the sampling. Jonny Horrox, Emma Chaney and Ashton Eaves have helped greatly during my time at the West Coast. I would also like to thank Jeroen de Klein from the Wageningen University for supervising me throughout the whole project.

Table of contents

1. Introduction

1.1 Problem definition

This thesis investigates how relatively high levels of coloured dissolved organic matter (CDOM) may influence the optical character, including light climate and possibly phytoplankton productivity, in Lake Brunner. Lake Brunner is the largest lake on the West Coast of the southern island of New Zealand at a distance of 30 km from Greymouth. The lake is classified as humic-stained and oligotrophic (Paerl and others 1979). This indicates that Lake Brunner contains low concentrations of nutrients and high concentrations of CDOM. Since 1992, Secchi depth, which is an indicator of visual water clarity, has decreased from 6.7 (mean in 1992) to 5.2 m (mean from 2005 to 2009). This decrease in Secchi depth can probably be attributed to an increase in phytoplankton productivity driven by a higher nutrient availability. Chlorophyll *a* is a measure of phytoplankton biomass, and its increase (slope of 0.040 mg m^{-3} yr^{-1}, median; 1.2 mg m^{-3}) seems to be a response to increases in epilimnetic phosphorus (slope of 0.103 mg m^{-3} yr^{-1}, median; 5.89 mg m^{-3}) and nitrogen (slope of 3.802 mg m^{-3} yr^{-1}, median;194.8 mg m^{-3}) (Verburg 2009; 2011; Verburg and others 2013a). Although Secchi depth has decreased, the current visual clarity is still high in absolute terms and in relation to guidelines (MfE 1994). However, if the increase in total phosphorus continues at the same rate the lake is expected to become mesotrophic by 2040, with consequently reduced visibility and ecosystem functioning (Verburg and others 2013a).

Reduced water clarity can potentially affect ecological structure and lake functioning in several ways. Firstly, increased light attenuation reduces (diffuse) light penetration with depth through the water column. This reduces photosynthesis at lower depths, and biological productivity of the lake ecosystem. Second, increased light attenuation reduces the visual range of sighted organisms. This affects, for example, predatory fish and birds which are dependent on sight for hunting prey (Belzile and others 2004; Davies-Colley and Smith 2001). Drastic changes in water clarity can be associated with a shift of the lake into an alternative state with a different ecosystem structure. Such a shift is hard to reverse (Scheffer and others 2001). Lastly, a change in water colour and clarity may impact the aesthetic appeal and suitability of the water body for recreational use (Davies-Colley and Vant 1987; Smith and others 1997).

CDOM has increased significantly over the period of 2003, the beginning of the measurements, to 2011, as did chlorophyll *a* (Verburg and others 2013a) as mentioned before. CDOM and chlorophyll *a* are both water constituents that attenuate light in the water column, and thus affect both aspects of water clarity. This may explain the decrease in Secchi depth over the last two decades. However, it is not clear to what extent Secchi depth is affected by either phytoplankton growth or concentrations of CDOM. An effect of high CDOM on water clarity might explain why Secchi depth is lower than expected with the current nutrient concentrations, which, in turn, affects light attenuation due to algae growth. However, CDOM absorbs part of the light that would otherwise be available for algal growth (Verburg 2011; Verburg and others 2013a). Therefore CDOM might also have a *positive* effect on visual clarity by inhibiting algal growth. Our hypothesis is therefore: **CDOM reduces light penetration and**

constrains phytoplankton biomass compared to what it might be if the nutrient loading could be fully 'realised', and thus lake Brunner is less sensitive than otherwise to nutrient enrichment.

To advise managers concerned with preventing further deterioration of water quality of Lake Brunner, more has to be known on the interactions between CDOM, chlorophyll *a*, phosphorus loading and light penetration. Also further insight into the inflow and retention of CDOM in the lake system is of importance. Therefore, photo-bleaching, the process by which solar UV light degrades CDOM, was also addressed in this research. The main question for this research, can be decomposed into a series of sub questions that elaborate the main question, as follows.

1.2.1 Main research question

Does CDOM inhibit the effects of eutrophication by limiting light availability for algal growth?

Is water clarity in Lake Brunner less sensitive to eutrophication than other lakes because of its high CDOM concentration?

1.2.2 Sub questions

- How does CDOM affect the algal biomass (chlorophyll *a*) and optical character of Lake Brunner and how do these attributes interact in their effect on water clarity?

  - How do CDOM and chlorophyll *a* : - affect light penetration (K_d(PAR)) in Lake Brunner?

    - affect visual clarity (Secchi depth) in lake Brunner?

  - How does CDOM affect chlorophyll *a* in lake Brunner by limiting light penetration?

  - How do visual clarity, CDOM and Chlorophyll *a* change in lake Brunner on a seasonal basis?

- Are the concentrations of CDOM in Lake Brunner in balance with the tributary inputs (meaning that the inflow and outflow mass of CDOM are equal, without accumulation or loss in the lake)?

  - What are the sources of CDOM in Lake Brunner? Which tributaries contribute most to CDOM inflow?

  - Does significant removal of CDOM by bleaching, or perhaps sorption and precipitation, occur within Lake Brunner (in summer[1]) such that its waters have lower CDOM than the flow-weighted mean of inflowing tributaries?

  - How does CDOM behave in lake tributary rivers? Is CDOM positively correlated with flow in inflowing tributaries – as has been reported for New Zealand rivers generally (Smith and others 1997) – such that higher flows deliver disproportionate humic matter to the lake?

[1] Note that, during summer the lake is stratified and the epilimnion isolated from the hypolimnion. Furthermore, in summer insolation is high compared to winter, so that photo-bleaching is probably more rapid. Both stratification and high solar radiation are likely to make bleaching more easily detected in summer.

-Is the epilimnion of Lake Brunner depleted in CDOM versus the hypolimnion during summer – due to reduced loading and/or removal processes, notably photo-bleaching of surface waters?

- ❖ Can an empirical model of reflectance be developed for lake Brunner? Reflectance relates to the brightness of water colour, which can potentially be observed by remote sensing. Humic stained waters, as lake Brunners, tend to be dark and have relatively low reflectance. Reflectance is mainly dependent on the ratio of backscattering to absorption. Can a relatively low reflectance be linked with high CDOM concentrations and low chlorophyll *a* concentrations? Can remote sensing potentially provide information about water quality?

  - Can reflectance and calculated values of absorption coefficient, *a*, and scattering coefficient, *b*, be linked to the water constituents in Lake Brunner.

  - Do calculated values of beam attenuation coefficient, *c*, equal values of *c* calculated through black disk measurements ($4.8/BD=c_{555}$)? This indicates whether the calculated values of c, by summation of *a* and *b*, are accurate, and can be used to check optical consistency of the dataset.

1.3 Literature review on light attenuation in natural waters

Water clarity of natural water is dependent on several optical properties controlling light attenuation. Firstly, there are apparent optical properties (AOPs), which depend both on the intensity and structure of the ambient light field, and the constituents of the medium. Secondly, there are inherent optical properties (IOPs) which only depend on the constituents of the aquatic medium and are independent of the ambient light field (Kirk 2011). Both visual clarity and light penetration into the water column are described by AOPs. The visual clarity of the water determines the sighting range through the water. Light penetration into the water column controls the light field of both phytoplankton and benthic aquatic plants. Visual clarity and light penetration are two distinct aspects of clarity. Knowing one does not imply knowing the other and vice versa (Davies-Colley and others 2014). Light is attenuated by either scattering or absorption of photons by water constituents. However, absorption can play a larger role in limiting light penetration as it actually extinguishes the photons, while scattering merely changes the direction of the photon (Kirk 1985). Scattering contributes to diffuse light attenuation by forcing the photons to take a tortuous path through the water column, resulting in an increased chance of absorption of the photon over a given depth interval (Davies-Colley and Nagels 2008). Figure 1 gives a graphical display of the conceptualisation of IOPs, when a light beam is transmitted through a water body.

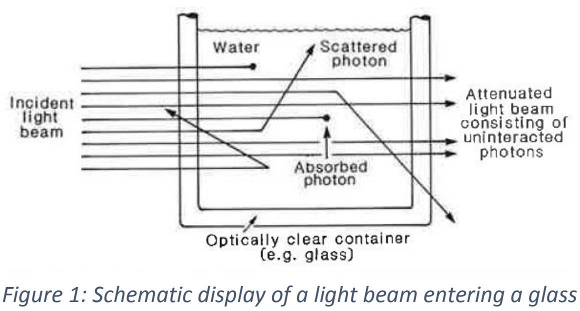

Figure 1: Schematic display of a light beam entering a glass of water, causing the photons to be scattered and absorbed (Davies-Colley 1978).

The total light attenuation by scattering and absorption is called the beam attenuation coefficient, c, and has the unit m^{-1}. This is thus the sum of the absorption coefficient, a, and scattering coefficient, b:

$$c = a + b \qquad (1)$$

These coefficients are IOPs and thus are only affected by the waters composition. The visual clarity of the water is inversely related to c, for example the Secchi depth is approximately 6/c (m^{-1}), although also affected (weakly) by the ambient light field (also shown in Eq. 3) (Zaneveld and Pegau 2003). Thus Secchi depth is considered an AOP.

The light penetration with depth is quantified by the diffuse irradiance attenuation coefficient, K, also with unit m^{-1}, defined as the proportional reduction of diffuse light per unit depth interval. This is an AOP, as it is dependent on the ambient light field (Davies-Colley and Smith 2001) as well as water composition. K can indicate attenuation in two major directions of irradiance, the downwelling irradiance attenuation coefficient (K_d) and the upwelling irradiance attenuation coefficient (K_u). K_u is a result of photons scattering in a backward direction, causing the photons to travel back towards the water surface. E_u, the upwelling irradiance is thus dependent on downwelling irradiance (E_d) and is thus always smaller. However E_u can become a contributor to photosynthesis when there is low absorption and high scattering in the water column. The ratio of upwelling irradiance (light in all directions) to down-welling irradiance is the reflectance, R:

$$R = E_u/E_d \qquad (2)$$

R is expected to be approximately proportional to the backscattering coefficient b_b, as most of the upwelling flux originates from backscattering. R is inversely proportional to the absorption coefficient a, which diminishes the amount of upwelling photons. R can be related to the brightness of water colour. Waters with low R tend to be dark, while a high R indicates bright colours. Brightness of water bodies can be observed by remote sensing, and can support water quality research by supplying information, for example, by indication water constituents (Davies-Colley and others 1988). Besides, combining R and K permits estimation of a and b, and thus c (Kirk 1994). Estimated values of c can be used to verify the optical consistency of datasets.

In the context of plant growth, the most relevant spectral distribution of light is the photosynthetically active radiation (PAR). This is the photon flux density (mol m^{-2} s^{-1}) in the 400-700 nm wavelength range (which is also the visible range for the human eye). The euphotic depth, z_{eu}, is defined as the depth where PAR falls to 1% of the irradiance level measured at the surface, and is a good indicator of the maximum depth at which photosynthesis is possible (Kirk 2011).

The Secchi disk is a widely used instrument to index visual water clarity. This black and white disk which is lowered into the water, until the white quadrants are no longer visible. This depth is called the Secchi depth. Secchi depth is inversely related to the sum of the beam attenuation coefficient (c) and the light attenuation coefficient (K) using the following formula (Davies-Colley and Smith 2001):

$$SD = G/(c + K) \qquad (3)$$

The unitless coefficient G depends on the reflectance of the white surface of the disk and the water reflectance, and usually lies between 6 and 9. However, c and K cannot individually be estimated from Secchi depth by using this equation without independent knowledge of the optics of the water body. K and c are only weakly related optical coefficients (Davies-Colley and Smith 2001). Although Secchi disk is widely used it has some disadvantages. First of all, the use of a Secchi depth is limited in rivers due to the shallow depth and the stream velocity. Secondly, the Secchi disk is an AOP, being itself dependent on K, and thus is slightly dependent on variations in the ambient light field. Because of these limitations, an alternative method of measuring visual water clarity has been developed, the (horizontal) black disk (BD) sighting range. As the disk is completely black, reflecting no light, it is only seen as a silhouette. The visibility of the black disk is therefore independent of the ambient light field, and can be classified as an IOP. The horizontal black disks visibility is inversely proportional to the beam attenuation coefficient and provides an estimate of this quantity (Davies-Colley 1988; Zaneveld and Pegau 2003), where c_{555} is the beam attenuation coefficient for light at 555 nm wavelength:

$$4.8/BD=c_{555} \tag{4}$$

As mentioned above, light in water can be attenuated by either scattering or absorption. The proportions in which light is scattered or absorbed is dependent on the constituents of the water. There are several types of constituents which scatter or absorb light in natural water; water molecules, dissolved organic constituents, and particulate constituents. Water molecules absorb red light strongly, but other coloured light weakly. This explains the blue colour of optically pure lakes. Water scatters light in a very weak manner. Of all the dissolved constituents, CDOM only causes light absorption (its scattering is negligible). CDOM, also referred to as yellow substance, is the main dissolved absorbent of light in water. CDOM especially absorbs light at blue and ultraviolet wavelengths, causing water, containing CDOM, to look yellow (Davies-Colley and Nagels 2008). Particulate matter may include phytoplankton, detritus and mineral solids. Phytoplankton scatters light strongly and selectively absorbs light for photosynthesis. This absorption is strongest at blue wavelengths. Phytoplankton gives water a green colour due to their photosynthetic pigments, mainly chlorophyll *a*. Organic detritus, tends to act similarly to CDOM regarding light absorption, imparting a yellow colour. However, organic detritus also scatters light. Finally, mineral solids are weak absorbers of light, but cause intense scattering of light (Davies-Colley 1978; Davies-Colley and Nagels 2008).

Photo bleaching of CDOM

In humic lakes, often more than 90% of the organic matter is in the form of dissolved organic matter (DOM), which is potentially important for the metabolism of microorganisms. However, typically most DOM is highly refractory to biochemical decay (being itself the metastable end product of bacterially-mediated biochemical decay), resulting in low bioavailability for microorganisms and slow degradation rates for DOM (Salonen and Vähätalo 1994). Furthermore, this refractory DOM is, to a large extent, condensed (polymerised) with delocalisation of electron fields resulting in light absorption over a wide spectral range, but typically rising in an exponential pattern with declining wavelength through the visible-UV spectrum (Davies-Colley & Vant 1987). The exponential absorption pattern imparts yellow colours to waters, hence the alternative name “yellow substance” and the acronym CDOM from coloured DOM. Furthermore, the yellow colour of CDOM is related to absorption of solar radiation which photo-catalyses the production of highly reactive oxygen species in water (e.g., singlet oxygen) – which, in turn, react with CDOM and oxidise some fraction to form inorganic carbon and water. In other words, CDOM auto-catalyses its own photo-destruction.

A study by Bastvinken et al. (2004) shows that between 5% and 24% of initial DOM concentrations were mineralised under different oxic and anoxic conditions over a period of 426 days, where oxic conditions stimulated the mineralisation of DOM. The incubation was conducted under dark conditions, and thus the degradation was not influenced by solar radiation. Solar radiation has the potential to alter the molecular properties of DOM, changing high weight molecules to more labile low weight molecules. DOM degradation by solar radiation occurs by either complete photo oxidation of the molecules or indirectly by altering the molecules to become bioavailable for bacteria (Bertilsson and Tranvik 2000; Dahlén and others 1996; Moran and Covert 2003; Salonen and Vähätalo 1994). By absorption of solar radiation the light-absorbing capabilities of CDOM is modified, resulting in less or no further light absorption. This process is called “photo-bleaching” and is caused by radiation in the ultraviolet (UV) and visible spectral region (Moran and Covert 2003). Radiation in the solar UV-A range (320-400 nm) is particularly important in promoting transformation of the structure, molecular weight, and optical properties of humic substances. When DOM is photo bleached it is transformed into dissolved inorganic carbon (DIC), carbon monoxide and low molecular weight molecules, such as carboxylic acids and aldehydes that are labile to bacteria (Bertilsson and Tranvik 2000). The study by Bertilsson and Tranvik (2000) suggests that DOM is more easily photo bleached in oligotrophic lakes such as Lake Brunner than in eutrophic lakes with high algal production because of generally higher levels of irradiance in the former. Apart from the ‘amount’ of UV absorbance (solar UV irradiance), the inherent properties of DOM and the attributes of the lake, such as pH, conductivity, alkalinity and iron content, may influence the transformation of DOM to DIC (Bertilsson and Tranvik 2000).

2. Methods

2.1 Physical geography of Lake Brunner

Lake Brunner is the largest lake on the West Coast of the South Island of New-Zealand, with a surface area of 41 km^2, a volume of 2.3 km^3, and a mean depth of 55 m. The mean hydraulic residence time (between 2000 and 2008) was 1.18 years (Spigel and McKerchar 2008). Figure 2 shows a map of the land-use of the catchment of lake Brunner. About 20 % of the catchment is used for agriculture (8 % is dairy farm). Most of the catchment is undeveloped native forest, and the lake is relatively unmodified (Verburg and others 2013a). Lake Brunner has three main tributaries, Crooked river, Orangipuku river and Hohonu river, and one outflow, the Arnold River. Furthermore, there are several smaller streams discharging into Lake Brunner which is regarded as rest inflow. The Carew is one of those streams. Table 1 shows the characteristics of the tributaries and other water sources.

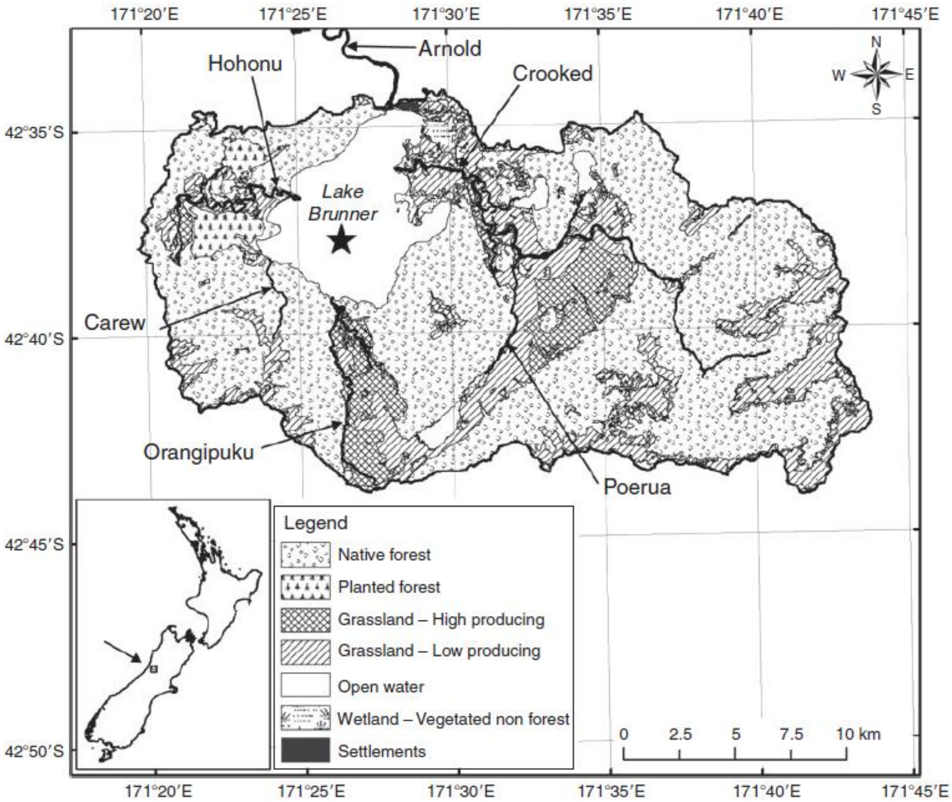

Figure 2: Land use in the catchment of lake Brunner, recorded in 2008 (Verburg and others 2013a).

Table 1: Water balance and catchment area of Lake Brunner as in 2008

Inflows	Water Balance *(%)* (Spigel and McKerchar 2008)	Estimated mean flow *(m^{-3} s^{-1})* (Rutherford and others 2008)	Catchment area *(km^2)* (Rutherford and others 2008)
Crooked River	49%	30.5	243
Orangipuku River	13%	8.0	45
Hohonu River	7%	4.2	46
Smaller streams and runoff	24%	15.2	106
Rain - evaporation (lake)	7%	3.6	41
Overall	100%	61.5	481
Carew (part of rest inflow)	1.1%	0.59	4.5

Verburg and others (Verburg and others 2013a) classify the lake as oligotrophic, which is defined by low concentrations of phosphorus (P) and chlorophyll *a*. Total phosphorus concentrations below 10 mg m^{-3} are classified as oligotrophic, which is the case for lake Brunner (mean P concentration = 6.5 mg m^{-3}). Paerl *et al.* (1979) suggested the lake is dystrophic. Dystrophic lakes are characterised by low to moderate planktonic production and high CDOM content, which give the water an amber-colour, and limit light penetration, inhibiting use of all available nutrients by phytoplankton. The DOM content is mostly allochthonous, meaning that it is produced at another location in the catchment and probably enters the lake via soil leaching and runoff. However, pH in lake Brunner is divergent from dystrophic lakes, being neutral instead of acid. Lake Haupiri is another humic stained lake on the West Coast, which is an clear example of a dystrophic lake. It is much smaller than Lake Brunner, and has maximum depth of about 20 meters. Furthermore, it has about 5 times higher CDOM concentrations than Lake Brunner, and productivity is low, despite it relatively high nutrients loading (see Table 2). Lake Brunner will be compared with Lake Haupiri, to compare with a more clearly dystrophic classified lake.

Table 2: Average values of variables, taken over a period of beginning 2010 till end of 2014, in lake Brunner and Haupiri.

	g340 (*m^{-1}*)	Total P *(mg m^{-3})*	Chlorophyll *a (mg m^{-3})*	Secchi depth *(m)*	TSS *(g m^{-3})*
Lake Haupiri averages (2010-2014)	33.31	13.38	1.33	2.22	1.77
Lake Brunner averages (2010-2014)	6.12	6.28	1.42	6.30	1.23

Phytoplankton growth in Lake Brunner is limited by P (Verburg and others 2013a) as was originally suggested by Paerl *et al.* (1979). Substantial increases in P and chlorophyll *a* since 1992 correlate with each other, where increased P seems to result in increased chlorophyll *a*. However no significant correlation has been found between increased N concentrations and chlorophyll *a* (Verburg and others 2013b). NH_4^+-N and NO_3^--N levels appeared to be high, relative to P concentrations, which is also consistent with P limitation of phytoplankton growth (Paerl and others 1979). Differences in mean N:P ratios between tributaries and the lake itself (respectively 46 and 69) show differential retention enhancing the limitation of P

(Verburg and others 2013b). Lake Brunner is thus vulnerable to changes in P, as there is a large difference between N and P concentrations relative to the stoichiometric demand of phytoplankton productivity (Verburg and others 2013a).

2.2 sub question 1: Interactions with Brunner's light climate

Water quality indicators in Lake Brunner have been monitored since 1992 by NIWA and later by the West Coast Regional Council. From 1992 to 1995, Secchi depth, chlorophyll *a* and total P have been monitored on a roughly bi-monthly basis. Between 2001 and 2009 these variables and additionally black disk, TSS, and absorbance have been irregularly monitored. From 2010 up till the end of 2014, the lake has been monitored monthly for all mentioned variables, and additionally upwelling and downwelling irradiance since 2011. Water samples have been collected using a 25 meter long tube, to integrate over the first 25 meters of the water column.

The data has been graphically checked for possible outliers, and these have been removed from the dataset. Four values of black disk and Secchi disk have been removed, as a black disk value can in theory not be larger than Secchi depth (Davies-Colley 1988). Furthermore one high outlier of total P, and two outliers with unrealistic low values of K_d have been removed. This has resulted in the following sample counts per variable measured in the mixed surface layer: Secchi depth (n = 124), black disk (n = 62), chlorophyll *a* (n = 139), Total P (n = 138), TSS (n = 93), g340 (n = 89), g440 (n = 89), g555 (n = 44), K_d (n = 39), K_u (n = 41).

The West Coast Regional Council has monitored Lake Haupiri on a bi-monthly basis, since the beginning of 2010. Data for Secchi depth (n = 28), g340 (n = 29), chlorophyll *a* (n = 29), Total P (n = 29) and TSS (n = 28) has been collected. No data has been removed regarding the statistical analysis.

Statistical analysis has been conducted with the program IBM SPSS Statistics 22. First, all data were checked for normality with a Shapiro-Wilk test, and transformed when needed by the use of Log-transformations. Multiple linear regressions (MLR) (either forward or backward) have been used to test for relationships between multiple variables. One-way Anova tests have been performed to compare means, and check for significant differences, and if found significant, followed up by a post hoc Tukey t-test. A p-value of 0.05 was used as significance level.

Theoretically, black disk would be preferable as the indicator for visual clarity, as it can be seen as an IOP. However due to more available and consistent data of Secchi depth than black disk in Brunner, and no black disk data available of Haupiri, it was chosen to mainly focus on Secchi depth as indicator for visual clarity.

A comparison study of lake Brunner and data from 119 New Zealand lakes, was used to check for deviations in chlorophyll *a* and visual clarity in Lake Brunner possible caused by CDOM. Averages per lake of chlorophyll *a* (n = 112), total P (n = 119) and Secchi disk (n = 69) were computed from data collected over the period from 2005 to 2009. This data was plotted, and the relative position of lakes Brunner and Haupiri in these plots compared to the regressions which can interpreted as possible effect of CDOM.

Whenever an estimate of dissolved organic carbon (DOC) was needed, the equation (5) by Collier (1987) was used, which was determined in multiple West Coast streams. This equation relates spectrophotometric absorbance, g340 (m^{-1}), to DOC (g m^{-3}). However, the accuracy of this equation is probably low, because it is not sensitive enough to indicate differences within a small range (range of equation 0 to 40 g m^{-3}) (Verburg 2011).

$$DOC = \frac{g340 * 0.596}{\ln 10} + 1.9 \tag{5}$$

2.3 sub question 2: CDOM balance

Auto sampling

There are three main tributaries (Crooked, Orangipuku and Hohonu) flowing into lake Brunner each of which supplies CDOM to the lake system. The inflow of each tributary has been evaluated by the instalment of an auto sampler, a sonde and hobo water level logger near the mouth of each tributary. The sondes and hobos were calibrated to measure turbidity, temperature, electrical conductivity and relative water level. These devices have been logging continuously, measuring every 15 minutes, over the period of 16 December 2014 till 12 March 2015, with a pause of 22 days in between, from 27 January till 18 February. The auto samplers were triggered manually to sample ahead of expected intense rain events. Once started, the auto samplers collected one sample every two hours over a period of 48 hours. Samples were preserved by cooling with ice (in the dark), to inhibit alteration of CDOM by bacterial activity or sunlight, until collection, and thereafter stored in a refrigerator. Not all samples could be used for analysis, due to limits of the budget. Therefore relevant samples were selected in the field by viewing the changes in the corresponding turbidity data. Changes in water level might have been a better indication for flow, however, due to lack of equipment in the field, this was not assessable at the times of collection. In total 68 samples have been collected (Hohonu n=21, Orangipuku n=23, Crooked n=22, and additionally Carew n=2). Auto sampling had been scheduled several times during the summer months. However, the summer was relatively dry (for the normally humid West Coast) and only two large events had been sampled by the beginning of March.

Collected samples were sent to the NIWA laboratory in Hamilton for analysis of spectrophotometric absorbance. CDOM can be indexed as the measurement of absorbance by dissolved matter in filtered water (0.45 µm membrane filter) at different wavelengths (340, 440 and 740 nm) using a spectrophotometer. Cells of 4 cm length were used for this measurement. The absorbance can then be converted to absorption coefficients g340 and g440:

$$g340 = \frac{\ln(10)\ (A340 - \left(\frac{740}{340}\right) A740)}{y} \tag{6}$$

$$g440 = \frac{\ln(10)\ (A440 - \left(\frac{740}{440}\right) A740)}{y} \tag{7}$$

where y is the cell length in meters, and residual scattering derived from near-infrared absorbance at 740 nm which is corrected for (Davies-Colley and Vant 1987).

Water balance

In order to calculate fluxes of CDOM, water flow data was required. However the sampling sites did not contain continuous water flow measuring stations. Therefore flow rates were calculated by the use of water level measurements by the hobos in the tributaries, and using a rating curve for the tributaries prepared by flow gaugings at different water levels. The water level recordings have been converted from relative to absolute level by the use of stage measurements at the site.

The Hohonu river was accessible and fordable during low to average flows. A rating curve has been created up till average flows. These flows have been calculated by step-by-step intersect measurements with an electromagnetic current meter (Marsh-McBirney), using equation (8):

$$Q = \sum_n \Delta w_n * d_n * v_n \qquad (8)$$

where Q is flow velocity ($m^3 s^{-1}$), w_n is the width of the section n (m), d_n is the depth of section n (m), and v_n is the flow velocity at 60% of the depth of section n ($m s^{-1}$).

The Crooked River was accessible, even during high flows, from a bridge, and thus a complete rating curve could be made. For the flow measurement an Acoustic Doppler Current Profiler (Streampro) was used. Unfortunately, the Orangipuku River was inaccessible and unfordable, and thus no rating curve could be made. The unknown flows of the Organipuku are established by the use of Crooked and Hohonu rating curves and the daily inflow data calculated from the water balance, as further described in the next section.

The total inflows into the lake have been roughly calculated by using the following water balance formula:

$$Inflow\ (I) + Precipitation (R) = Outflow\ (O) + Evaporation\ (E) + Water\ level\ change\ (\Delta H) \qquad (9)$$

The lake outflow into the Arnold River and lake water level are both continuously recorded at Moana. Precipitation was estimated by taking the average of the rain gauge at Arnold river station (north of lake Brunner) and Pigeon Creek near Inchbonnie (south of Lake Brunner). Evaporation has been estimated using the simple Abtew-Method which uses solar radiation to estimate daily lake evaporation (Abtew and Melessa 2013):

$$E = K_1 \frac{R_s}{\lambda} \qquad (10)$$

where E is evapotranspiration (mm day^{-1}), R_s is solar radiation (MJ m^{-2} day^{-1}), λ is latent heat (MJ kg^{-1}) and K_1 is a dimensionless coefficient (0.53). This equation has been found the most accurate in a study of eight different radiation-based evaporation equations (Xu and Singh 2000). The closest meteorological station to Lake Brunner that measures solar radiation is the Pigeon Creek station.

CDOM balance

The CDOM balance was constructed by combining the logged water levels (to convert water level to water flow), rating curves and CDOM plots (measured CDOM *versus* estimated flow) by which the Crooked and Hohonu CDOM inflows were estimated. The daily water flow rates of the Crooked and Hohonu rivers were subtracted from the daily inflow estimated from the water balance (Eq. 9) to estimate Orangipuku and rest inflows. Subsequently, the percentages of the three computed components of the daily inflow were calculated relative to the total inflow. Using the ratios between the three main tributaries found by Spigel and McKerchar (2008), a new relative water balance was computed. The Orangipuku inflow was then calculated from its proportion relation to the Hohonu and Crooked rivers. Rest inflows fluctuates much due to rain events, while the Orangipuku has a more stable flow rate. Whenever the calculated Orangipuku inflow surpassed $inflow_{rest\,+\,orangipuku}$, $inflow_{rest\,+\,orangipuku}$ was taken as the inflow of the Orangipuku. Rest inflows were calculated as the residual part, after all three tributaries were subtracted from the total inflow. Rest inflow was of interest as it forms a large part of the total inflow (Fig. 3) and is also a source of CDOM. Unfortunately, the rest inflow consists of many small streams, and thus individual monitoring of each stream was too elaborate.

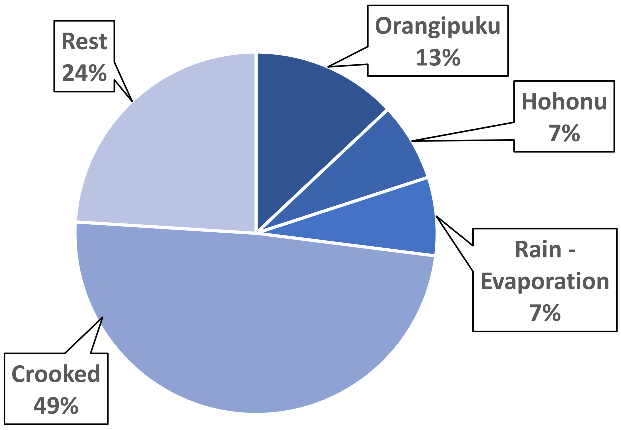

Figure 3: Overview of all water inflows of Lake Brunner calculated by Spigel and McKerchar (2008).

The CDOM *versus* flow graph of the Orangipuku was computed by plotting daily average flows against daily averages of the auto sampling results. In addition, prior existing WCRC data of the flow rates of the Orangipuku river were used.

Also, Crooked and Hohonu rivers water flows during days without logged water levels (60 days of total 120 days) were estimated with the computed water balance, and mean proportions of each river in the balance, to calculate daily means for each tributary.

No stage measurements were performed regarding the logged water levels of the Hohonu in December and January. The logger had been replaced in between the first and second logged period, and thus the relative logged water levels were incomparable. Daily average inflow from February and March of Crooked were plotted against Hohonu daily average inflows of this period (Fig. 4). The regression line equation of this plot and the Crooked flow estimates of December were used to estimate inflows of Hohonu in December and January.

Subsequently water level (WL) was back calculated from these estimated inflows, using the Hohonu rating curve. The average difference between the calculated WL and measured WL was used to adjust the measured WL to actual WL. Hohonu daily inflows were recalculated and updated in the original Crooked versus Hohonu plot (Fig. 4), resulting in a updated regression line equation. This process was repeated until no change occurred in the equation, resulting in a correlation with $R^2 = 0.75$.

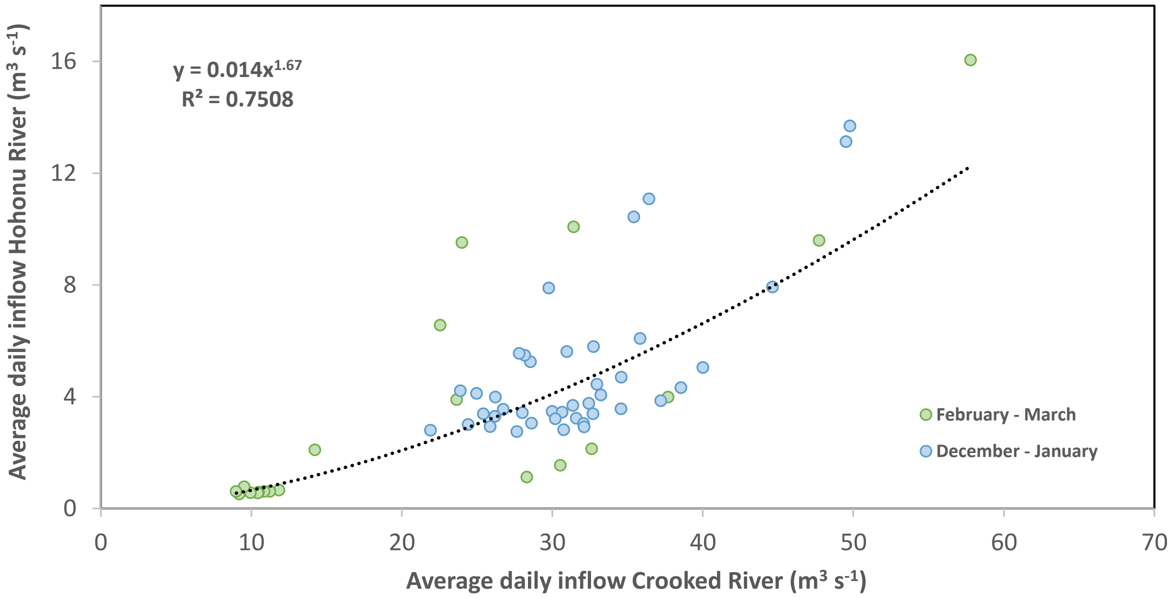

Figure 4: Average daily inflows for Crooked and Hohonu. This plot was used to calculate relative water level to actual water level.

Photo-bleaching

Hypothetically, CDOM might be out of balance between Lake Brunner and its catchment inflows owing to CDOM loss processes, including sunlight photo bleaching, sorption on solids and sedimentation, and bacterial metabolization. To investigate the possibility of photo bleaching, an in situ experiment has been conducted. An installation of five lines, with six 50 ml quartz test tubes attached to each line at different depths (0.5 ,1, 2, 3, 4 and 5 meters), were installed in the centre of the lake over the period of a month. The euphotic depth in Lake Brunner is about 9 meters, and we originally expected UV-A radiation to penetrate less than PAR by about 2-fold hence the experimental depth range[2]. The tubes were made of quartz to allow transmission of UV radiation (Salonen and Vähätalo 1994). Their orientation was upside down, to prevent shading by bottle caps. The tubes were filled with unfiltered lake water originating

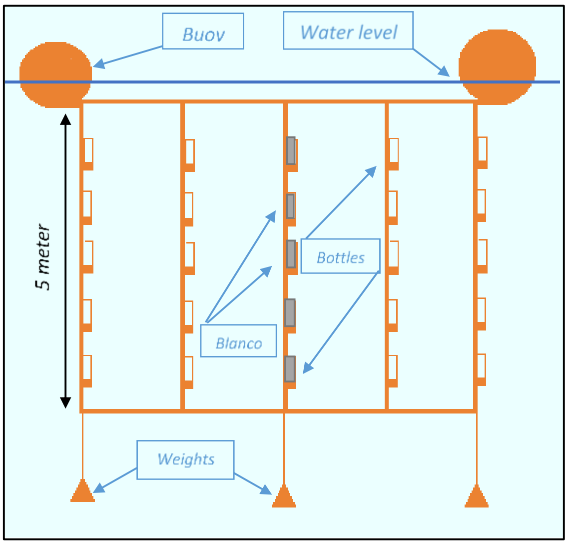

Figure 5 overview of bleaching experiment setup

[2] Results show that actual UV-A radiation penetration is much less than expected, as will be elaborated further on.

from a 15 meter depth and sealed off before lowering into the water column. 15 meters had been chosen, as CDOM was most likely less affected by photochemical decay, being below the UV-A radiation penetration limit. The collected lake water had been mixed thoroughly before filling up the tubes, to ensure similar CDOM starting concentrations among the tubes. An additional sample from the same container used to fill the bottles was taken, as the initial CDOM concentration (t=0). The tubes on one of the lines were covered with aluminium foil, to exclude light. Figure 5 gives a graphical overview of the experimental setup. The experiment was planned to last three consecutive months during summer. However, entanglement of the lines confounded the first experiment in December, and the experiment could only be resumed in February. This has resulted in only one instalment over the period of 17 February 2015 till 19 March 2015. After collection of the samples, they were send to the laboratory for analysis of spectrophotometric absorbance and processed as for tributary auto samples.

Stratification
A sample was taken each month from both the epilimnion (15 m) and the hypolimnion. Sample depths of the hypolimnion differed per month; December 95 m, January 40 m, February and March 70 m (which was the middle of the hypolimnion in February and March). These samples were also analysed on absorbance. Additionally, in February, both epilimnion and hypolimnion samples were analysed on particulate organic carbon (POC).

Longitudinal variation in CDOM
Each of the main three tributaries of Lake Brunner had its contributing streams sampled and analysed for absorbance. This was only done for the lower catchment of the tributaries as the rivers are inaccessible in the mountains and the water seemed to be low in CDOM based on sightings of the upper reaches. The Hohonu River was sampled at seven locations on the 4th of March, once at the autosampler site, once at the beginning of the lower catchment, and five locations upstream along the river. The CDOM concentration at the auto sampler site was adjusted, using the water level at time of sampling along the transect, as the transect could not be completed in one day. The Crooked River was sampled on the 10th of March, at seven locations, once at the autosampler site, once at the beginning of the lower catchment, at four sites at the confluence with inflowing streams and one at Lady Lake, which was the source of a stream that was otherwise unreachable. The Orangipuku river was sampled at four locations, once at the autosampler site, and at three other locations along the river.

2.4 sub question 3: Reflectance model

All formulas in this section originate from Kirk (1994), apart from equations 17 to 21 (Kirk 2011).

Since May 2011, up till the end of 2014, upwelling and downwelling irradiance (respectively, E_u and E_d) profiles at the central lake Brunner site have been measured on a monthly basis using two cosine quantum PAR sensors. These sensors were placed in opposite orientations, to measure both up- and downwelling irradiance. The first measurement was taken near surface and the instrument was subsequent lowered at one meter intervals until downwelling irradiance levels approach zero. From these profiles, the downwelling and upwelling irradiance attenuation coefficients (K_d and K_u) were computed using equations (11) and (12).

$$K_d = -\frac{\partial \ln E_d}{\partial z} = -\frac{1}{E_d}\frac{\partial E_d}{\partial z} \qquad (11)$$

$$K_u = -\frac{\partial \ln E_u}{\partial z} = -\frac{1}{E_u}\frac{\partial E_u}{\partial z} \quad (12)$$

It follows from these equations, that the slope in a plot of E_d or E_u on a ln-scale against depth gives K_d or K_u. Additionally, K_ε, the net downward irradiance (E_d-E_u) has been calculated in a similar way as K_d and K_u;

$$K_\varepsilon = -\frac{\partial \ln (E_d - E_u)}{\partial z} = -\frac{1}{(E_d - E_u)}\frac{\partial (E_d - E_u)}{\partial z} \quad (13)$$

Reflectance (R) can be calculated as the ratio between upwelling irradiance and downwelling irradiance, according to formula (14):

$$R = E_u \, / \, E_d \quad (14)$$

An average R has been computed for each light profile over the depth range where the surface irradiance decreased to 1%. Below this depth, the measurements deviate increasingly and were unreliable. Near surface deviating R values, or other outliers, have also been removed from the average calculations, to compute more accurate R values. Four average R values have been completely removed from the analysis, as their individual calculated R values fluctuated greatly.

Absorption and scattering coefficients *a* and *b* (both IOPs) cannot easily be measured, and are more conveniently calculated from more easy measurable variables, Ku, Kd and R (all AOPs). Equation (15) allows absorption coefficient, *a,* to be calculated from underwater irradiance functions, solar altitude and the coefficient G_E, which accounts for the scattering phase function of the water.

$$\alpha = \mu_0 K_\varepsilon(z_m) \left\{ \frac{1 - R(z_m)}{1 + R(z_m)[103 G_E(\mu_0) - 1]} \right\}^{1/2} \quad (15)$$

Coefficient G_E can be assumed to be similar in most waters and can be determined by equation (16).

$$G_E(\mu_0) = 0.473\mu_0 - 0.22 \quad (16)$$

The cosine of the refracted solar photons just beneath the water surface, μ_0, is a requisite for both equation *(15)* and *(16)*, can be obtained by equations *(17)* to *(21)*. Equation *(17)* calculates the solar declination, δ, via ψ, which expresses date by an angle (ψ = 360° * d/365; d = day number, ranging from 0 on 1 January to 364 on 31 December). The equation contains a negative sign to correct for the southern hemisphere.

$$\delta = -(0.39637 - 22.9133 \cos \psi + 4.02543 \sin \psi - 0.3872 \cos 2\psi + 0.052 \sin 2\psi) \quad (17)$$

Equation (18) uses the solar declination, δ, the latitude, y (42.6167° for Lake Brunner), and τ (calculated by 360° * t/24; t = hours elapsed since 00:00h) to calculate solar elevation, β.

$$\sin \beta = \sin y \sin \delta - \cos y \cos \delta \cos \tau \quad (18)$$

From solar elevation, the solar zenith angle, θ_a, can be calculated following equation (19):

$$\sin \beta = \cos \theta_a \quad (19)$$

From the calculated solar zenith angle, θ_a, the angle of refracted photons just beneath the water surface can be calculated, θ_w, using Snell's law (20). For this purpose, a value of 1.33 for the ratio n_w/n_a is close enough for light of any wavelength in the PAR-range in freshwater.

$$\frac{sin\theta_a}{sin\theta_w} = \frac{n_w}{n_a} \qquad (20)$$

Finally, the cosine of the angle of refracted solar photons beneath the water surface gives the needed μ_0 for the equations (15) and (16), and is shown in (21). After finding *a*, the scattering coefficient *b* can be computed by equation (22) and beam attenuation coefficient *c* can be calculated by summing up *a* and *b*.

$$\cos\theta_w = \mu_0 \qquad (21)$$

$$\frac{b}{a} = \frac{103R(z_m)}{1-R(z_m)} \qquad (22)$$

The variables, R, *a, b*, and *c,* were statistically analysed as dependent variables in MLR analyses with chlorophyll *a*, g340 and TSS as independent variables.

3. Results

3.1 Results sub question 1: Interactions with Brunner's light climate

Results of the first sub question, which is centred mainly around lake Brunner, will be addressed here . However results from monitoring of visual clarity in lake Haupiri will also be shown throughout this section.

- How does CDOM affect the algal biomass (chlorophyll *a*) and optical character of Lake Brunner and how do these attributes interact in their effect on water clarity?

Visual clarity – Secchi depth

A multiple linear regression (MLR) analysis with Secchi depth as dependent factor and g340, chlorophyll *a*, and TSS as independent factors, showed the individual effect of each independent variable on the variability in the dependent variable. p-values given as a results of MLR analyses are partial coefficients. Variable TSS was rejected as a predictor of Secchi depth ($p = 0.167 > 0.05$). g340 had a p-value that was above the confidence level ($p = 0.077 > 0.05$) and theoretically should thus be rejected. However as the p-value was close to the confidence level it was decided to retain g340 part of the model. Chlorophyll *a* was significantly affecting Secchi depth ($p < 0.0001$). The model is therefore a combination of chlorophyll and g340, as can be seen in Eq. 23 with a R^2 of 0.273. Figure 8 shows the measured Secchi depth values plotted against the modelled Secchi depth values. Figure 6 and 7 show the individual relation of Secchi depth with chlorophyll *a* or g340, without correction of the effect by the other variable on Secchi depth.

$$Secchi\ depth = 10.244 - 2.015\ Log\ chlorophyll\ \mathrm{a} - 5.545\ Log\ g340 \qquad (23)$$

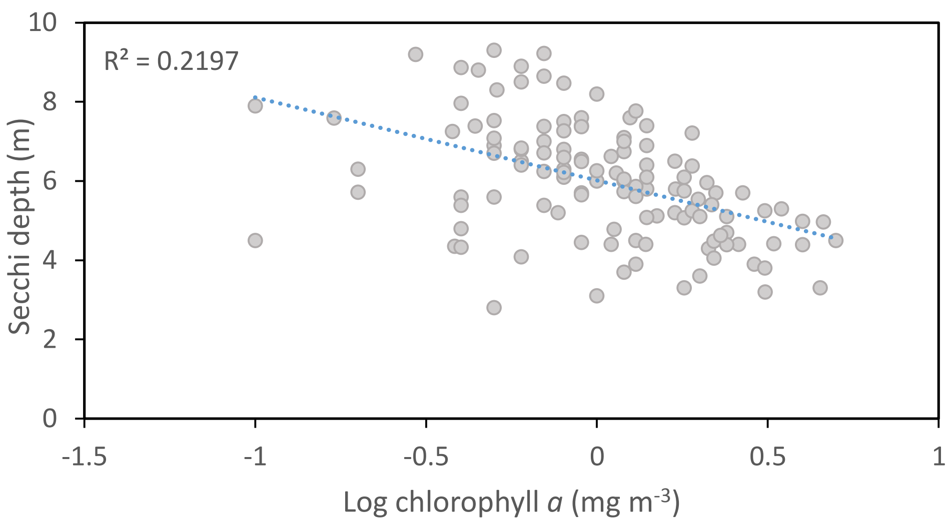

Figure 6: Secchi depth plotted on a logarithmic scale against chlorophyll a *with $R^2 = 0.2197$*

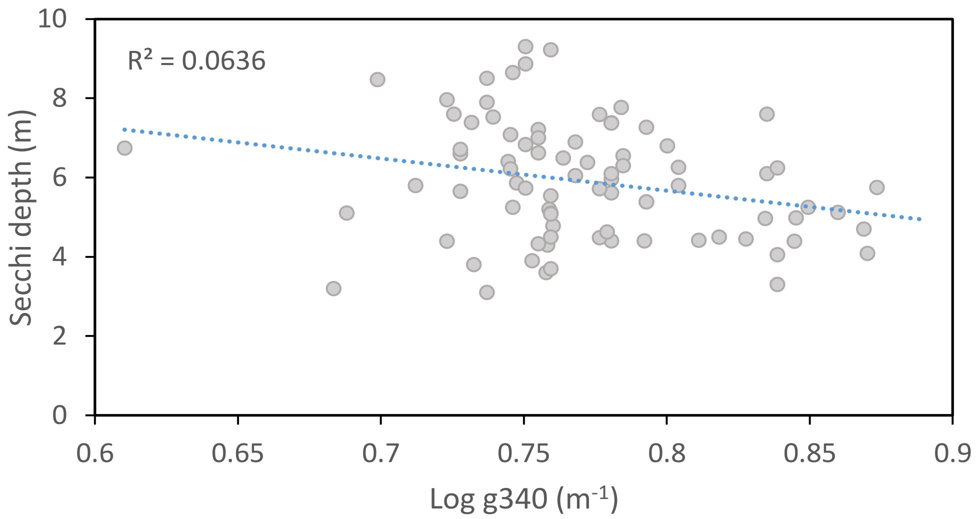

Figure 7: Secchi depth plotted on a logarithmic scale against g340 with $R^2 = 0.0636$

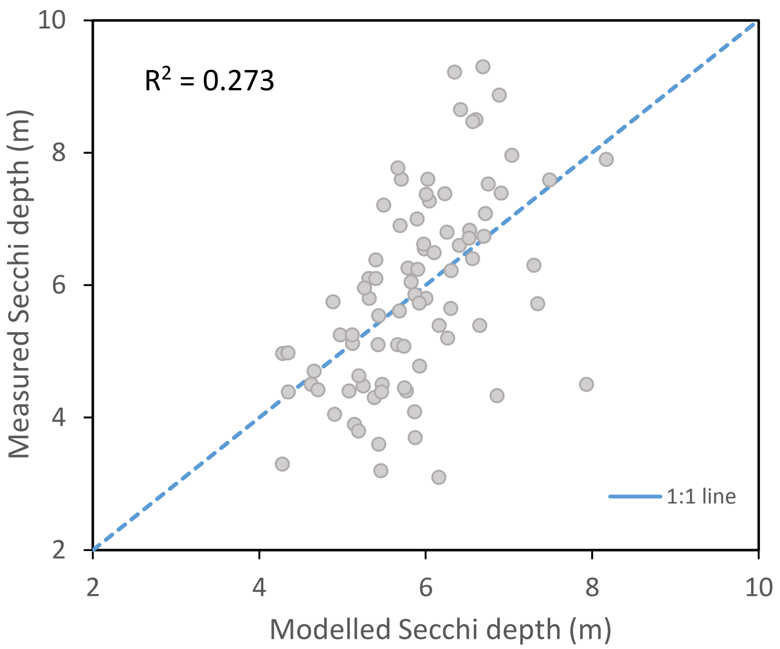

Figure 8: Measured values of Secchi depth plotted against Secchi depth modelled by eq. 23 with measured values of chlorophyll a *and g340 (R = 0.273)*

Visual clarity – Black disk

From equation 4, c_{555} can be calculated from black disk. Furthermore, following from equation 1, $c_{555} = a_{555} + b_{555}$, with absorption and scattering coefficients at 555 nm. As absorption is affected by water, CDOM, and chlorophyll, the absorption coefficient, at 555 nm, can be estimated with : $a_{555} = a(\text{water})_{555} + a(g)_{555} + a(\text{chlorophyll})_{555}$

Therefore g555 should contribute to visual clarity measurements by black disk, unlike g340 and g440. MLR with dependent factor black disk and independent factors chlorophyll *a* and either g340, g440 or g555 showed that g340 and g440 were not a significant (respectively, $p = 0.656 > 0.05$, $p = 0.468 > 0.05$) predictor for black disk. However, as expected, g555 and chlorophyll *a* both affected visual clarity, measured by black disk, significantly (respectively, p

= 0.035 < 0.05, p = 0.0004 < 0.05) resulting in equation 24. Figure 9 shows the accuracy of the model, plotting measured values against modelled values of black disk.

$$Log\ Black\ Disk = 0.459 - 0.198\ Log\ chlorophyll\ \mathrm{a} - 0.291 \log g555 \qquad (24)$$

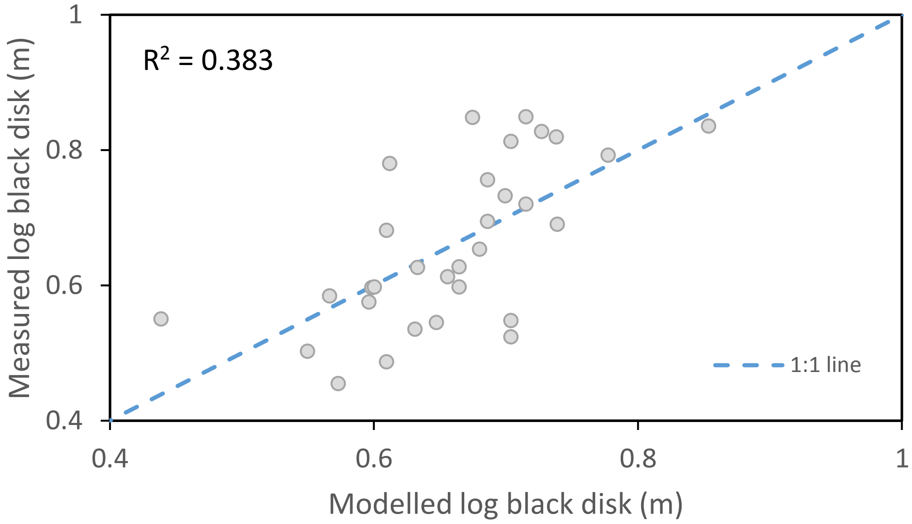

Figure 9: Measured values of black disk plotted against values of black disk modelled by eq. 24 with measured values of chlorophyll a *and g555, (R = 0.383)*

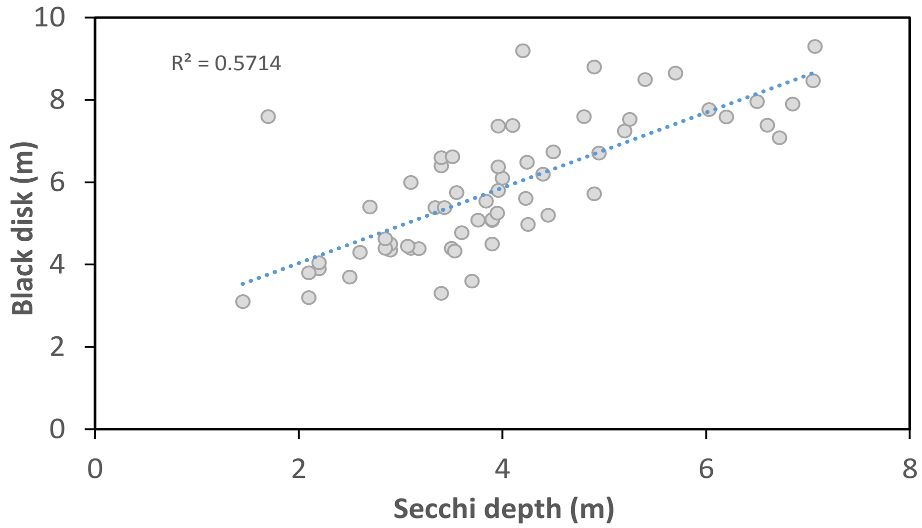

Figure 10: The two indicators for optical clarity plotted against each other to check for consistency in the data.

Light penetration - K_d

Lastly, MLR analysis with dependent factor K_d, and independent factors chlorophyll *a* and, g340 or g440 showed that chlorophyll *a* (p = 0.064 > 0.05) was nearly significantly correlated, and g340 was significantly correlated with K_d (p = 0.02 > 0.05). However the constant value of the computed linear model was not found significant (p = 0.728 > 0.05). Therefore the linear model with g340 would not be accurate to predict K_d. A regression with g440, on the other hand, was able to compute a more accurate linear model for K_d. The constant, g440, and chlorophyll *a,* are all significantly correlated with K_d (respectively p < 0.0001, p = 0.022, and p = 0.051). This results in the model (25) with R^2 = 0.198. Figure 11 and 12 show the regressions with K_d by the two variables individually. Figure 13 shows the accuracy of the model.

$$K_d = 0.523 + 0.74 \log chlorophyll\ \mathrm{a} + 0.541 \log g440 \qquad (25)$$

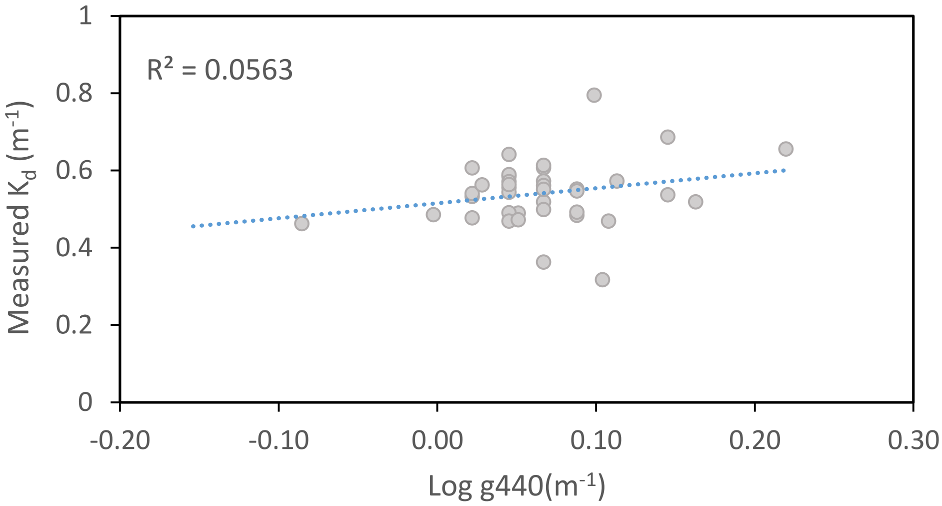

Figure 11: K_d plotted on a logarithmic scale against g440 with $R^2 = 0.0563$

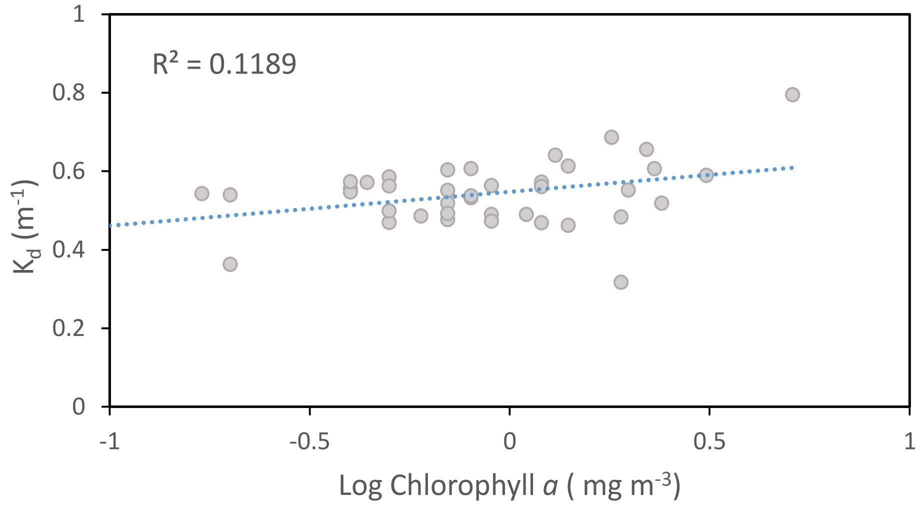

Figure 12: K_d plotted on a logarithmic scale against chlorophyll a *with $R^2 = 0.1189$*

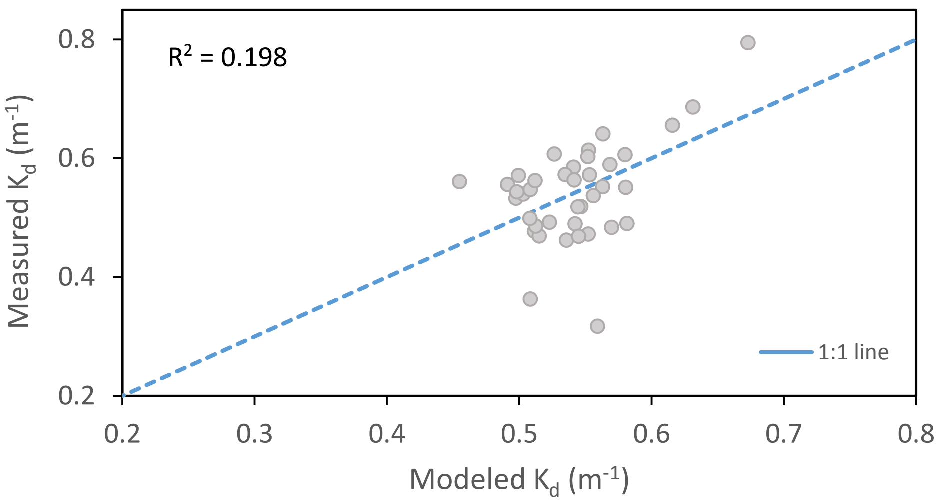

Figure 13: measured values of K_d plotted against values of K_d modelled by eq. 25, with measured values of chlorophyll a *and g440 (R = 0.198)*

Visual clarity - Lake Haupiri

Lake Haupiri is more humic-stained than Lake Brunner (about 5.5 times higher mean of g340 absorbance), and contains on average almost double the concentration of total P. Remarkably, the average chlorophyll *a* concentration in lake Haupiri is almost the same or even lower than lake Brunner, despite the much higher phosphorus concentration (Table 2).

A MLR analysis was also conducted for Secchi depth in Lake Haupiri. Secchi depth was the dependent variable, and g340, chlorophyll *a*, and TSS[3] were the independent variables. In this case chlorophyll *a* was rejected from the regression ($p = 0.978 > 0.05$). This leaves a regression with g340 and TSS to predict Secchi depth with a R^2 of 0.571 (respectively; $p = 0.001 < 0.05$, $p = 0.001 < 0.05$). The model is shown in Figure 14. Equation (26) gives the predictive model:

$$Secchi\ depth = 3.794 - 0.045\ g340 - 0.727\ log\ TSS \qquad (26)$$

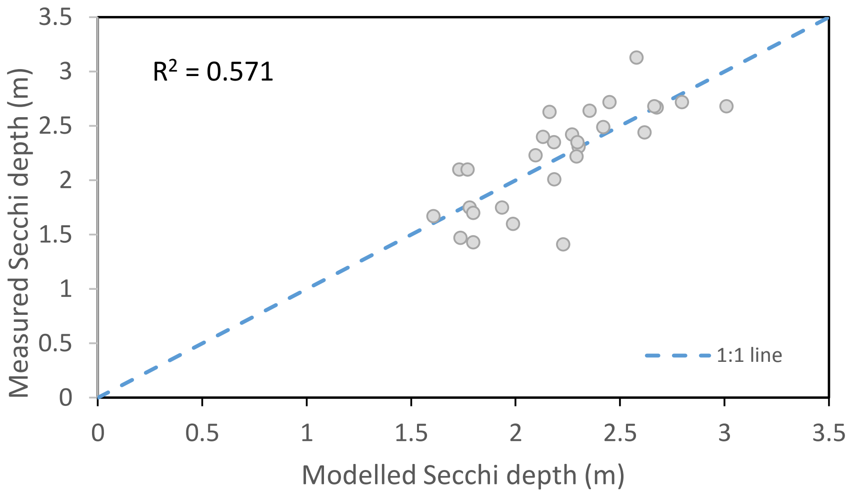

Figure 14: Measured values of Secchi depth in Lake Haupiri plotted against values of Secchi depth modelled with measured values of TSS and g340 by eq. 26 (R = 0.571)

Effects on Chlorophyll *a*

Lake Brunner

To assess the possible limiting effect of CDOM on chlorophyll *a*, a MLR analysis has been conducted with chlorophyll *a* as dependent variable and, total P and CDOM (either g340 or g440) as independent (predictor) variables. 440 nm is the wavelength at which chlorophyll absorbs most light for photosynthesis, and thus if any competition occurs, it might be best shown by g440 (Menken and others 2005). However, the analysis removed both g340 ($p = 0.314 > 0.05$) and g440 ($p = 0.448 > 0.05$) from the models, leaving a model predicting chlorophyll *a* by total P alone ($R^2 = 0.09$, $p < 0.001$). This model is given by formula 27 and is shown in Figure 8.

$$Log\ chlorophyll\ \mathrm{a} = -0.536 + 0.748\ Log\ total\ P \qquad (27)$$

---

[3] Phytoplankton (indexed by chlorophyll *a*) is part of TSS, and is therefore not exactly independent as MLR assumes. However, bivariate correlation between chlorophyll *a* and TSS shows no significant correlation ($p = 0.861$), thus both variables are kept in the MLR analysis.

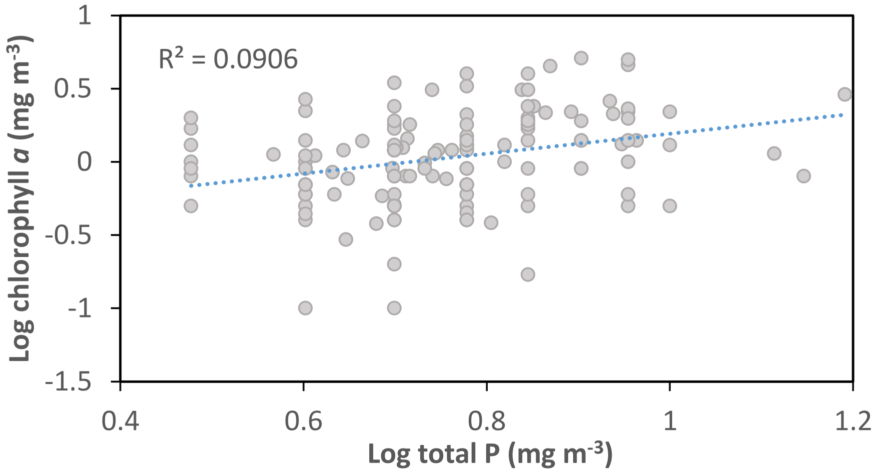

Figure 15: Regression of chlorophyll a *against total P* on a logarithmic scale

Lake Haupiri

The higher concentrations of CDOM in lake Haupiri might have a stronger effect on chlorophyll *a*, compared to lake Brunner. MLR analysis, with chlorophyll *a* as dependent and g340 and total P as independent variables, removed g340 from the regression model ($p = 0.332 > 0.05$). Total P was also significantly correlated with chlorophyll *a* ($p = 0.014 < 0.05$) leading to equation 28. Remarkably, total P seems to be inversely related to chlorophyll in Lake Haupiri, unlike Lake Brunner.

$$\text{Log chlorophyll a} = 2.119 - 1.873 \text{ Log total P} \qquad (28)$$

Comparing lake Brunner and lake Haupiri with New Zealand lakes

Addressing the potential limiting effect of CDOM on chlorophyll *a* was also tested by comparing Lake Brunner and Lake Haupiri to New Zealand as a whole. Average values of Secchi depth, total phosphorus and chlorophyll *a* of 119 new Zealand lakes over the period of 2005 – 2009 are plotted in figure 16, 17, and 18. This resulted in a regressions between those variables, giving an overview of the general trends. The location of lake Brunner and Haupiri in the graphs allows examination of deviations from general relationships among lakes, which might be explained by the relative high CDOM concentrations. The values for lake Brunner were average values over the period of 2005 till 2014. Lake Haupiri's values were averages of 2010 till 2014. Lake Haupiri is positioned below the regression line in all plots. This also true for Lake Brunner in Figure 17 and 18. However, figure 16 (Chlorophyll *a* against total P) shows lake Brunner positioned on the regression line. Standard error bars are added for lake Brunner and Haupiri, but are fairly low. Standard error bars can only clearly be seen clear in figure 18.

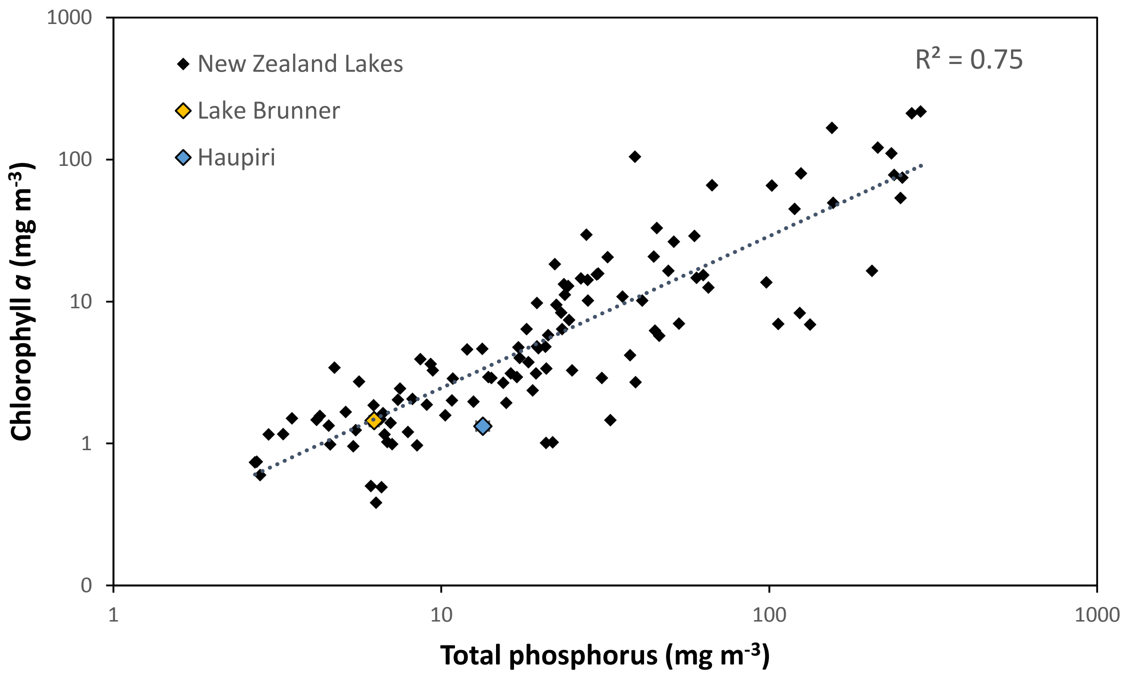

Figure 16: Chlorophyll a *plotted against total phosphorus for 119 New Zealand lakes. Lake Brunner is indicated by a yellow point, Lake Haupiri by a blue point.*

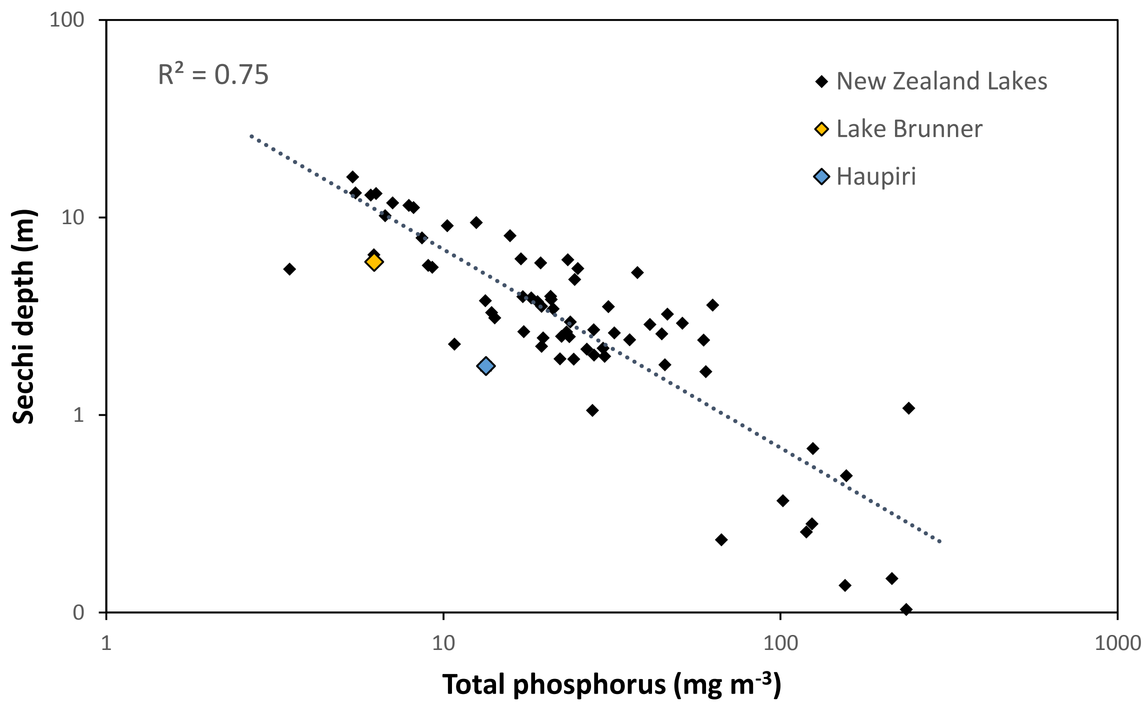

Figure 17: Secchi depth plotted against total phosphorus for 119 New Zealand lakes. Lake Brunner is indicated by a yellow point, Lake Haupiri by a blue point.

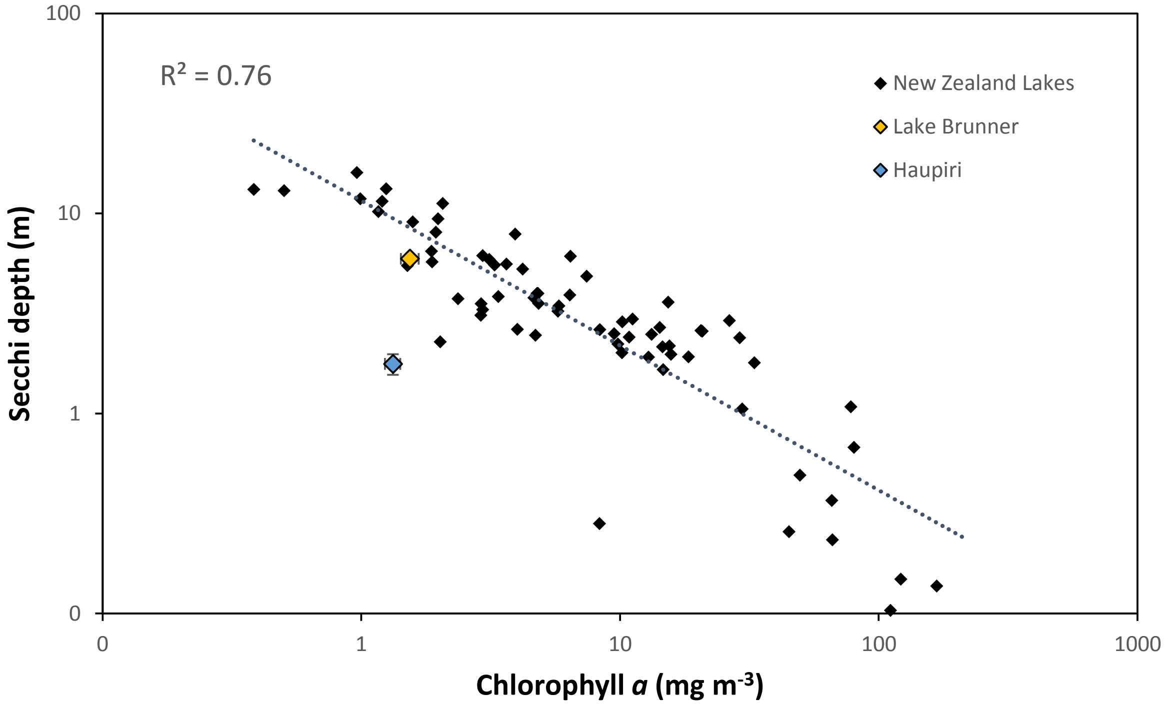

Figure 18: Secchi depth plotted against Chlorophyll a *for 119 New Zealand lakes. Lake Brunner is indicated by a yellow point, Lake Haupiri by a blue point. Standard error bars are shown for both lake Brunner and Haupiri.*

Seasonality

Chlorophyll *a*, g340, total phosphorus, and the measures for light penetration and visual clarity (Secchi disk, black disk, K_d and reflectance) were statistically analysed to see if there is any differences between seasons. This has been done by comparing seasonal means, performing an one-way ANOVA test. This shows that only the seasonal means of chlorophyll *a* ($p < 0.001$), g340 ($p < 0.05$), and reflectance ($p < 0.05$) are significantly different between seasons. Further investigation, doing an Tukey t-test, shows that for g340, the means of spring and summer ($p < 0.001$), and spring and autumn ($p < 0.05$) were significantly different. For chlorophyll this is true for winter compared to all the other seasons ($p < 0.001$ for all). Finally, the mean for autumn for reflectance is significantly different from those for summer and spring (both $p < 0.01$). Table 3 gives an overview of the seasonal means for all of the variables and the p-values. Figure 19 gives a graphical display of the variables that contain significantly different means.

Table 3: Overview of seasonal means with p value for results of oneway ANOVA test; Those in blue are have significantly different from those in green.

	Chlorophyll *a* (mg m^{-3})	g340 (m^{-1})	Reflectance (-)	Secchi disk (m)	Black disk (m)	K_d (m^{-1})	Total P (mg m^{-3})
p-value	0.000	0.005	0.010	0.096	0.070	0.588	0.580
Winter	0.71	5.84	0.0078	6.46	4.37	0.51	5.81
Spring	1.47	5.64	0.0077	5.99	3.58	0.57	6.17
Summer	1.57	6.27	0.0094	5.51	3.52	0.57	6.19
Autumn	1.53	6.10	0.0047	6.06	4.45	0.55	5.75
Total	1.34	6.06	0.0073	5.98	4.02	0.54	5.99

There were no significant differences in seasonal means for Secchi depth and black disk, although p-values are close to the confidence level of 0.05. Figure 20 shows graphs of the seasonal means of Secchi depth and black disk, and their standard deviation error bars.

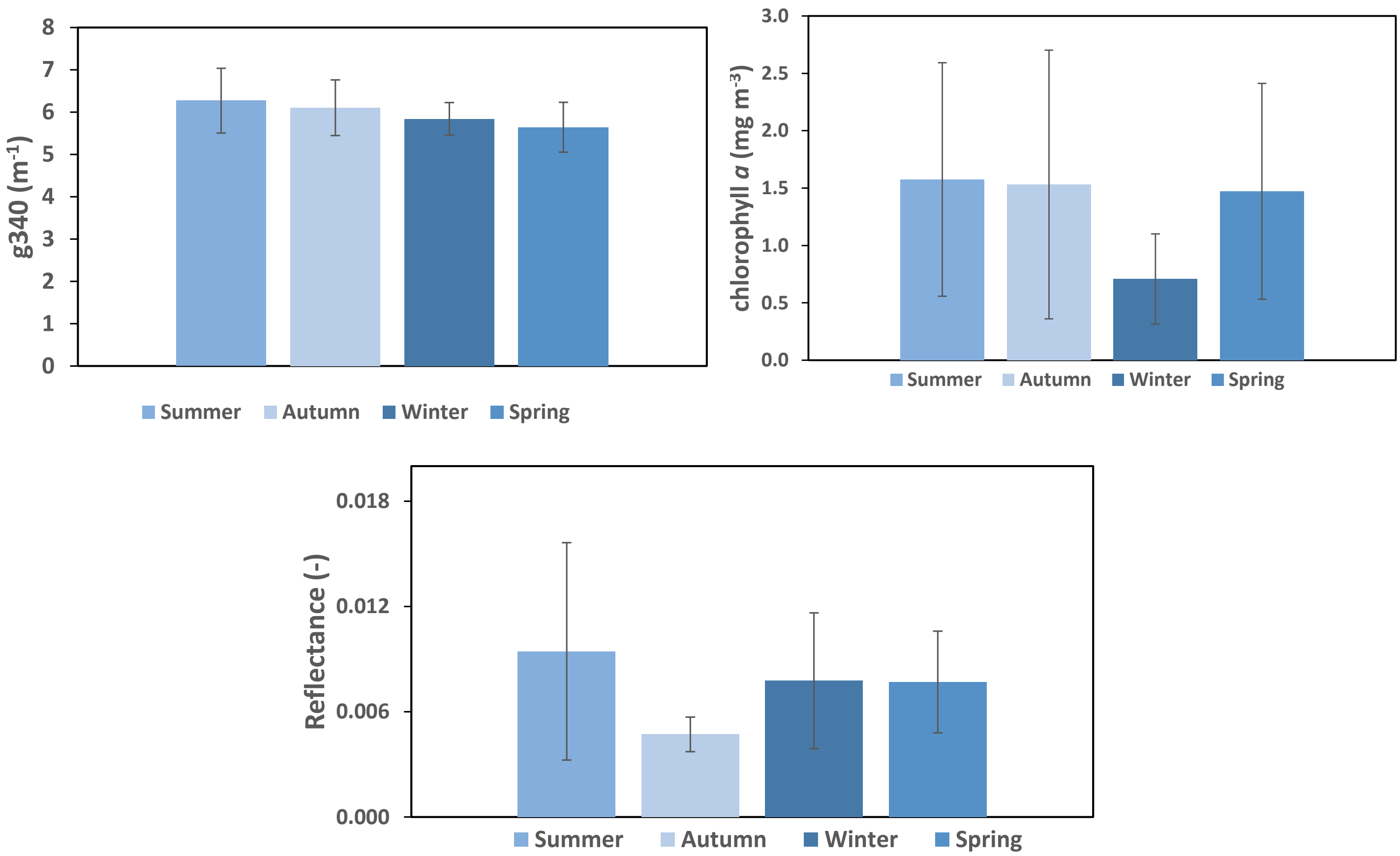

Figure 19: Display of the variables chlorophyll a*, g340 and reflectance, which have significantly different means for some seasons (shown in table 3). Error bars show standard deviations.*

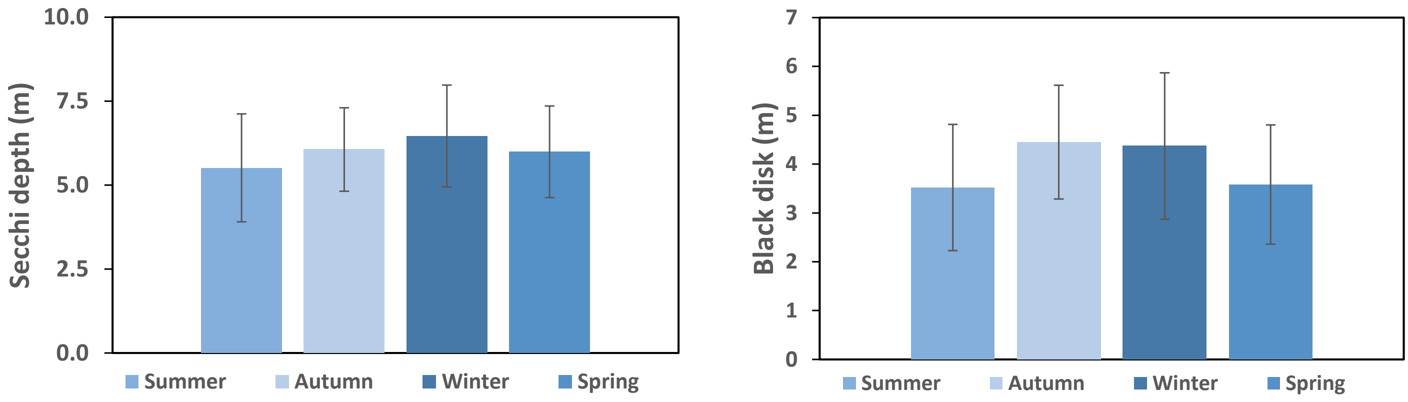

Figure 20: Overview of average per season of visual clarity indicators Secchi disk and black disk. No significant difference between seasonal means have been found. Error bars show standard deviations.

Changes over time

A similar method has been applied to the annual means. All variables, apart for reflectance, have significant different means between the years, according to the One-Way ANOVA test. P-values can be seen in Figure 14. This figure also indicates which years have significantly different means compared to others. Again blue years are significantly different from green years. Chlorophyll has several years which are significantly different from other years. These differences have additionally been displayed by yellow and dark green. Total P is the only variable which has no individual significant different annual means.

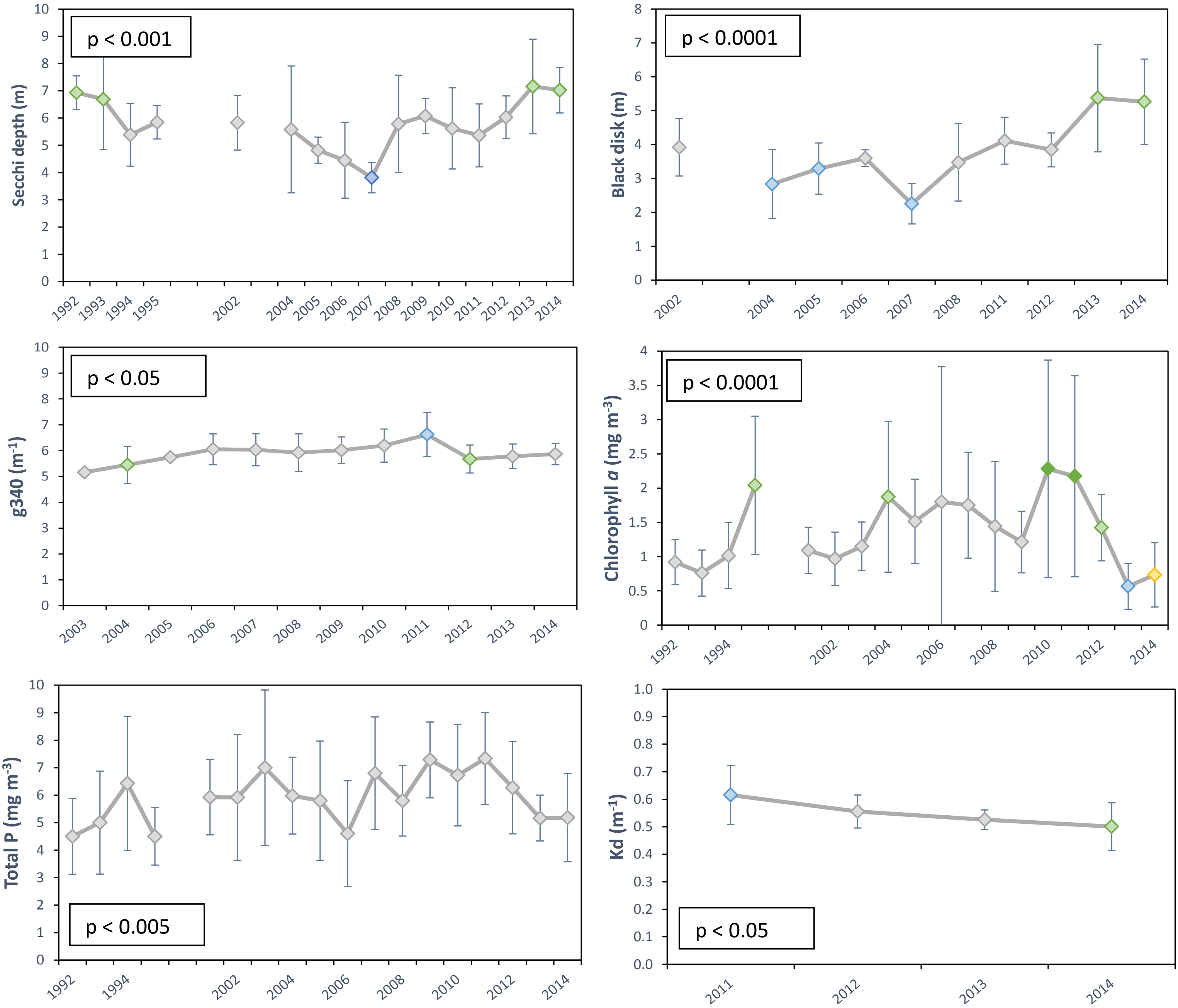

Figure 21: Annual means for all variables that have significantly different means (p values given in graph). Grey points have no significant different means. Years with blue points have significant different means compared to the green points. Years with yellow points have a significant different mean compared to the dark green points. Error bars show standard deviations.

3.2 Results sub question 2 : The CDOM balance

In this section the results are given to answer the sub question below. First, the results needed to calculate the CDOM balance are given in section 3.2.1 summer water balance, 3.2.2 rating curve, 3.2.3 Temperature, 3.2.4 CDOM versus flow, 3.2.5 CDOM bleaching, 3.2.6 stratification. In section 3.2.7 all these results are combined to calculate the final summer CDOM balance. Section 3.3.8 is a small side project to investigate sources of CDOM in each tributary transect.

- ❖ Are the concentrations of CDOM in Lake Brunner in balance (meaning that inflow and outflow amounts are equal to each other, without accumulation or loss in the lake)?

3.2.1 Summer water balance

Below, Table 4 shows the water balance during the summer. Figure 22 displays the computed average daily inflow of the four months. High inflows were present at the start of summer, which decreased over the months, due to low precipitation in the catchment. Inflow peaked again in March after several heavy rain events, which was at the time of the auto sampling.

Table 4: Computed summer water balance.

	In				Out				
	Inflow (m^3)	+	Precipitation (m^3)	=	Outflow (m^3)	+	Evaporation (m^3)	+	Lake level change (m^3)
December	1.87E+8	+	1.19E+7	=	2.38E+8	+	5.16E+6	+	-4.46E+7
January	1.26E+8	+	5.18E+6	=	1.42E+8	+	6.25E+6	+	-1.71E+7
February	9.73E+7	+	5.63E+6	=	1.03E+8	+	4.34E+6	+	-4.48E+6
March	1.53E+8	+	1.25E+7	=	1.54E+8	+	3.17E+6	+	7.75E+6

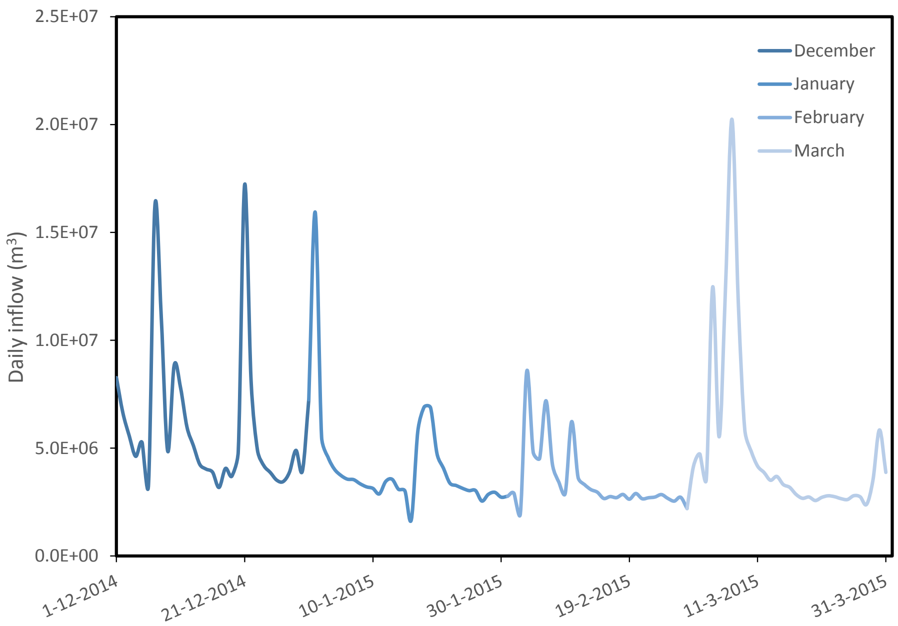

Figure 22: Overview of change in outflow over the summer from 1-12-2014 till 31-03-2015

Table 5 gives an indication of the relative importance of each tributary of the total flow. The percentages have been calculated using the manufactured rating curves and water level data of the Crooked and the Hohonu, and old percentual inflow data (Spigel and McKerchar 2008), which has been adjusted by removing 'rain – evaporation' .

Table 5: Recalculated relative inflow per tributary

Tributary	Relative inflow (%)
Crooked	48.8
Hohonu	7.6
Orangipuku	12.8
Rest	30.8
Total	100

3.2.2 Rating curves

In Figure 23 the rating curves of the Crooked (left) and the Hohonu (right) can be seen. The rating curve for the Orangipuku could not be made due to inaccessibility of the river. Measurements were made over the period of 17 February till 13 March. The green measuring point in the Crooked rating curve was measured about two months after the other measurements, and might therefore be less accurate if a changing riverbed changed the flow dynamics of the river over the two intervening months.

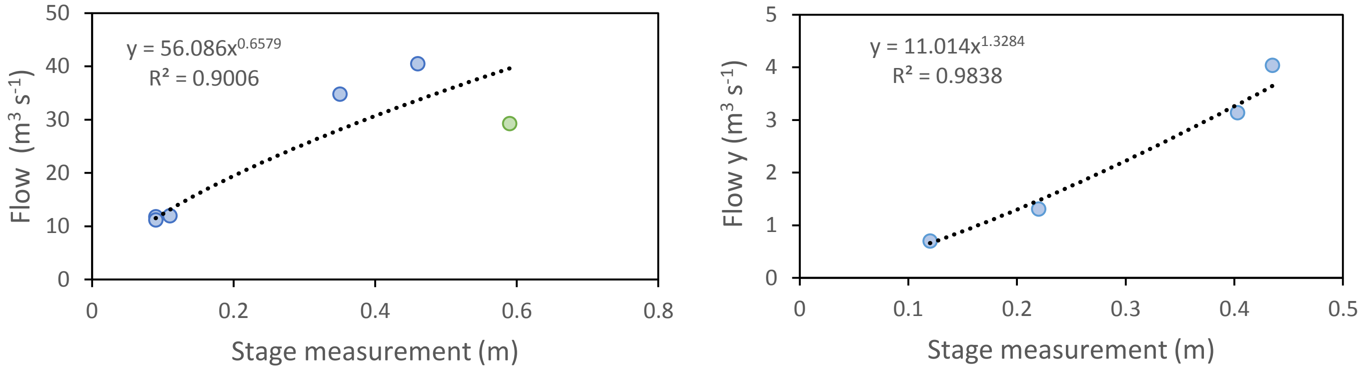

Figure 23: Rating curves for Crooked river (left) and Hohonu river (right). Stage length was an additional 0.63 m (Crooked) and 0.32 m (Hohonu) for total water level.

3.2.3 Temperature

Figure 24 shows the temperatures of the tributaries during the logged periods. Additionally, for each month a temperature profile of the lake has been made resulting in the temperatures for the lake surface, the start of the thermocline and the hypolimnion. The dotted lines are estimates for changes in those temperatures assuming a linear increase. As the tributary inflow temperatures are all above the hypolimnion temperature, it is expected that no inflow enters the hypolimnion. This indicates that the hypolimnion is isolated from any CDOM inflow during these summer months, and all CDOM ends up in the epilimnion and thermocline region.

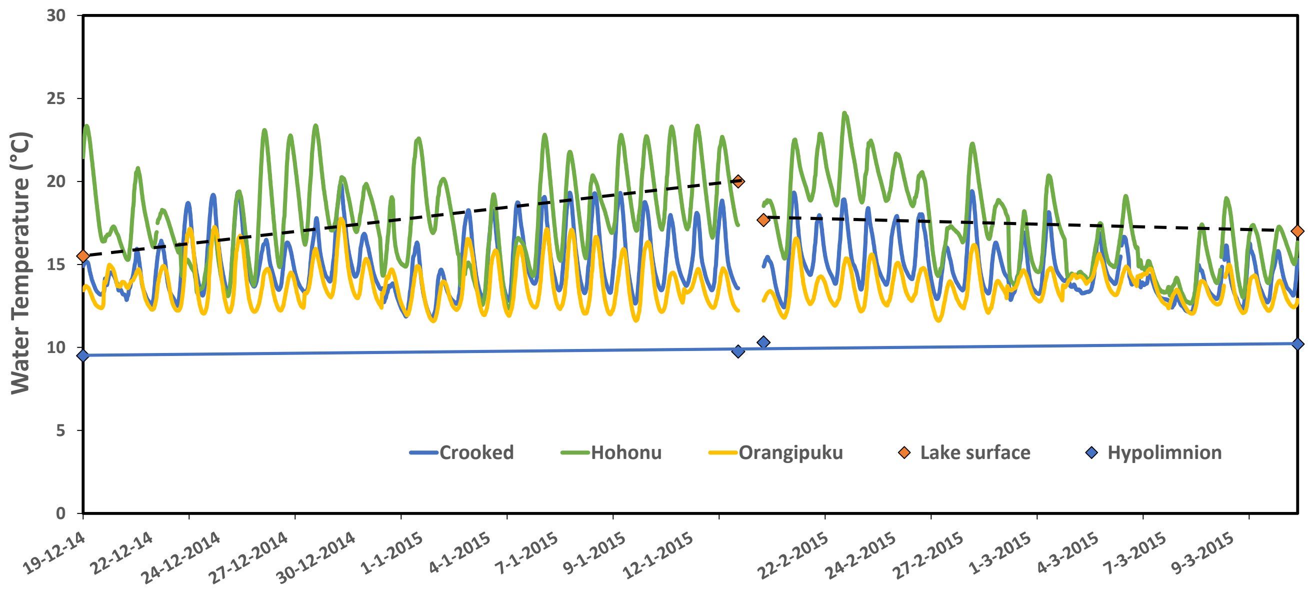

Figure 24: Logged water temperatures in tributaries from 19 December 2014 till 11 march 2015. Note that Temperature data is missing from 14 January till 20 February. Lake temperature is only measured once every month, and is thus only shown at the start and end of each logging period. The dotted line is only an indication of temperature change in the lake.

3.2.4 CDOM *versus* flow

Figures 25, 26, and 27 show the results of the auto sampling experiments. The Crooked and the Orangipuku graphs show two sampling events, where the first starts at zero hours and the second at around 40 hours. The Hohonu graph shows only one sampling event, which is the same as the second event in the other graphs. The dotted line shows a possible trajectory in CDOM concentration during time spans where no sampling was done. Note that the graph of the Orangipuku shows turbidity as an estimate for flow velocity in view of the missing rating curve.

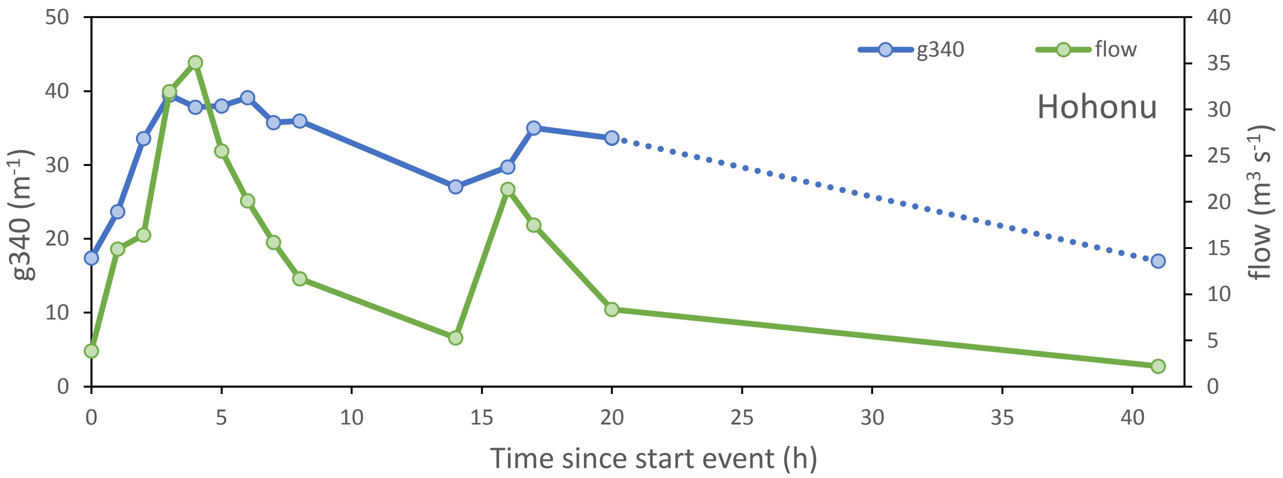

Figure 25: Flow velocity and g340 of the Hohonu river plotted over time during an intense raining event and the aftermath. Hour 0 is on 6-3-2015 and hour 40 is on 9-3-2015

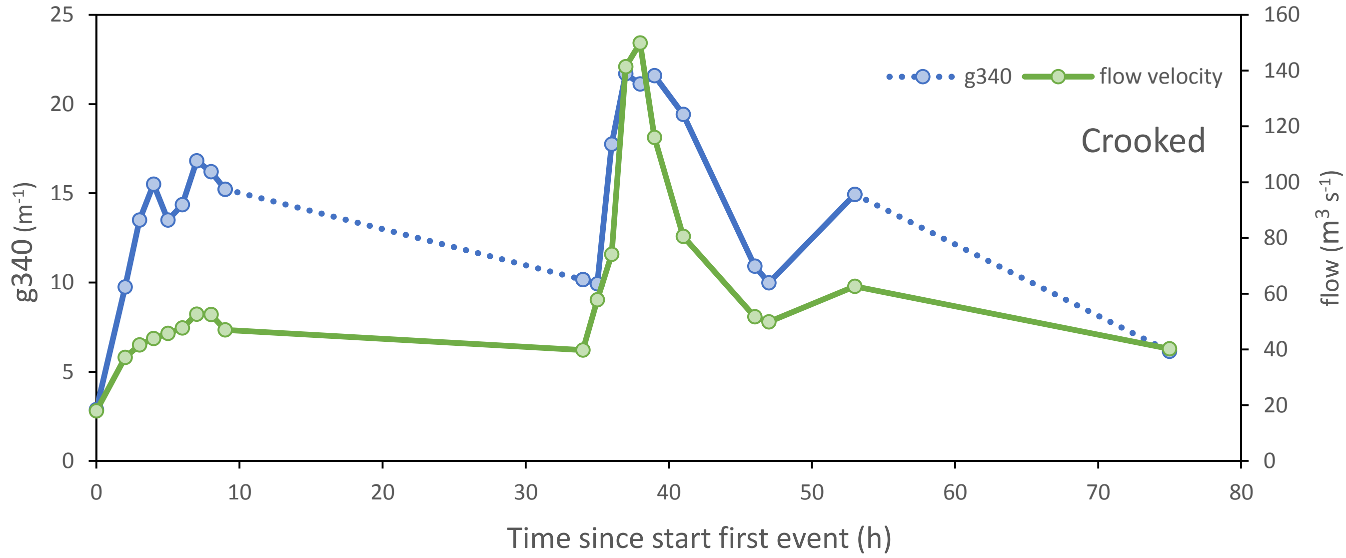

Figure 26: Flow velocity and g340 of the Crooked river plotted over time during two intense raining events and their aftermaths. Hour 0 is on 3-3-2015, hour 75 is on 9-3-2015

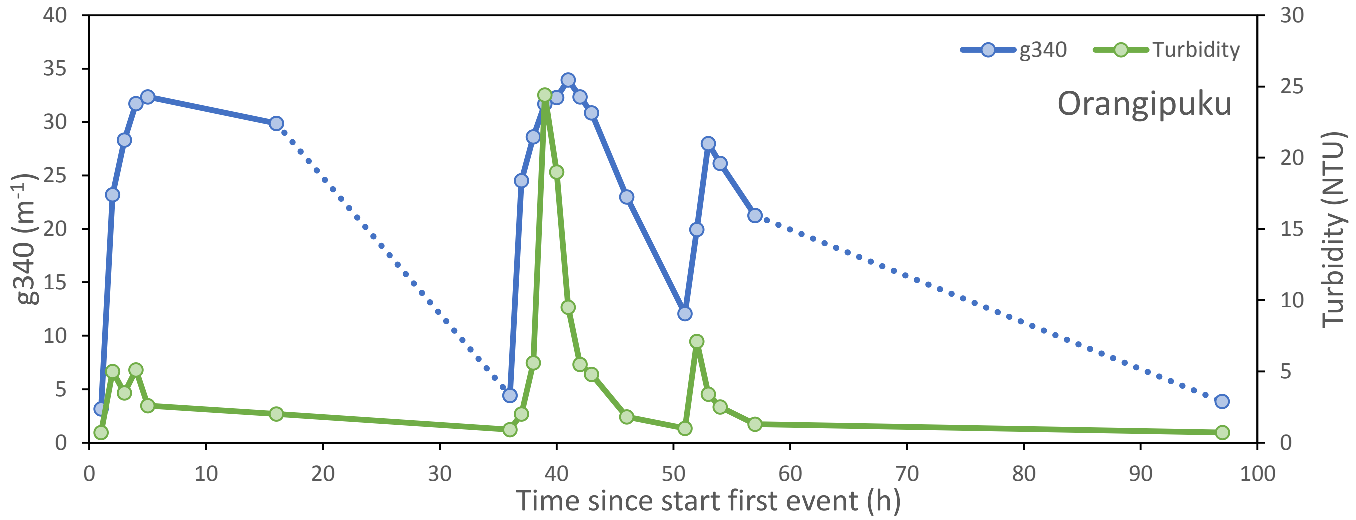

Figure 27: Flow velocity and g340 of the Orangipuku river plotted over time during two intense raining events and their aftermaths. Hour 0 is on 3-3-2015, hour 75 is on 9-3-2015.

The graphs above only show one or two events which occurred closely. Figure 28, 29 and 30, include more data points and events than shown above and plot g340 *versus* flow. The Crooked and Hohonu graphs consists of data collected by the WCRC (respectively, n = 24 and n = 26), which are single measurements of flow and CDOM throughout 2011 till 2014. The data from December consist of a small rain event (Crooked, n = 2, Hohonu, n=6). February - March consists of the events described in the graphs above and several single measurements around these events (Crooked, n = 21, Hohonu, n=16). The Orangipuku graph also include of data from WCRC (n = 28). However, for the Orangipuku, CDOM concentrations from February – March are daily means. As flow measurements were not possible, average daily flow velocities computed by a water balance were used (n = 7).

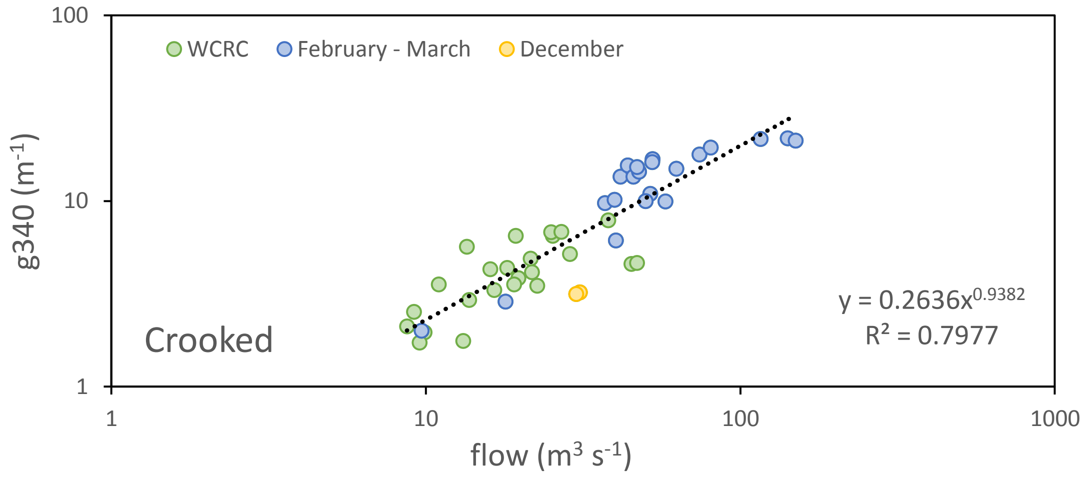

Figure 28: g340 is plotted against flow for Crooked river.

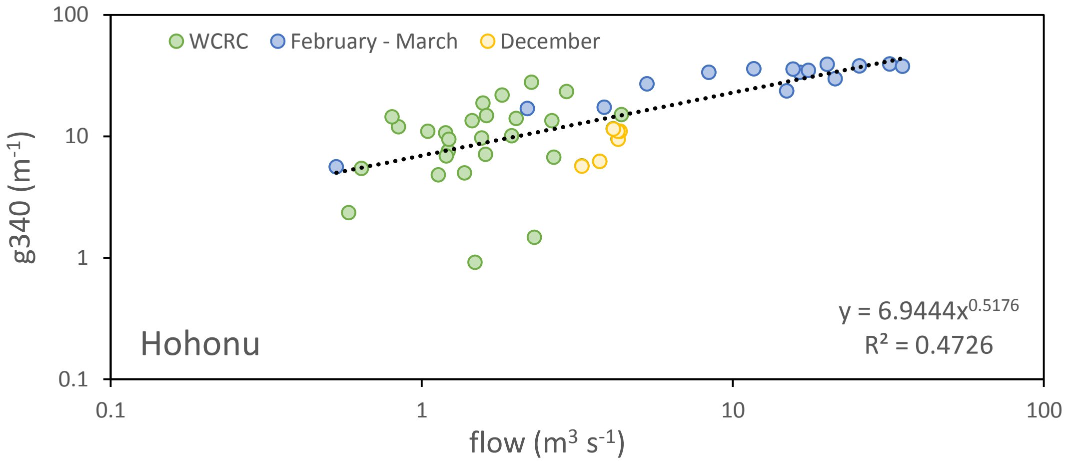

Figure 29: g340 is plotted against flow for Hohonu river.

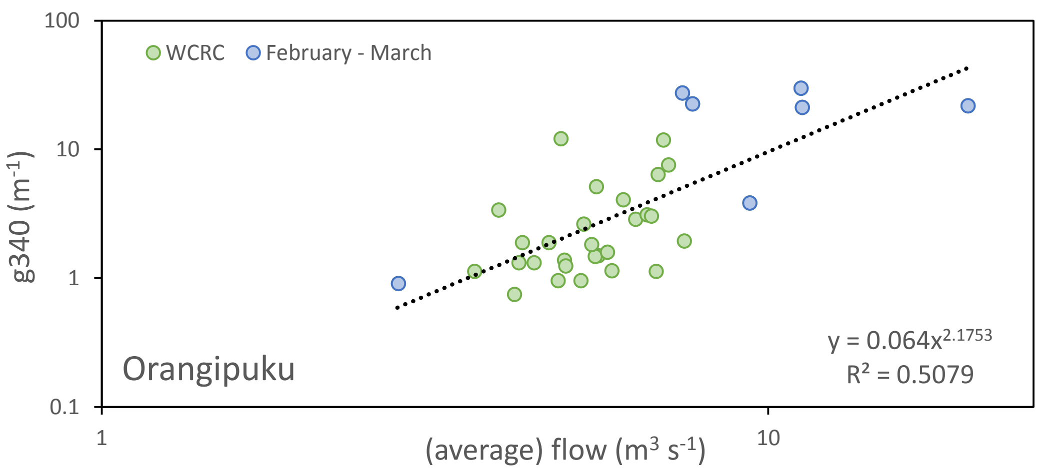

Figure 30: g340 is plotted against flow for Orangipuku river. Flow and g340 coefficients from February – March are daily averages.

3.2.5 CDOM Bleaching

Table 6 shows the data of the bleaching experiment's first run from February till March. Initial g340 absorbance at the start of the experiment was 6.4 (m^{-1}). The depths of the bottles were not identical, due to small errors in fabrication of the alignment. Standard deviations of identical depths were however low, ranging from 0.03 to 0.06 m. Bottle 6 of line 2 has been removed from the analysis as the value of g340 is an outlier. Data of g440 has not been used in the analysis, as the ratio between g340 and g440 seems to have a high variability compared to other g340 and g440 data. This can be seen in Figure 34 in the appendix. Figure 31 displays the data in a graph, where g340 absorbance is plotted against depth.

Table 4: Absorbance data results of bleaching experiment installed over the period of 17-2-2015 at 11:00 till 19-3-2015 at 11:45.

Initial g340 value:	6.40

Line 1			Line 2			Line 3 (unexposed)			Line 4			Line 5		
Depth (m)	*g340 (m^{-1})*	*g440 (m^{-1})*	*Depth (m)*	*g340 (m^{-1})*	*g440 (m^{-1})*	*Depth (m)*	*g340 (m^{-1})*	*g440 (m^{-1})*	*Depth (m)*	*g340 (m^{-1})*	*g440 (m^{-1})*	*Depth (m)*	*g340 (m^{-1})*	*g440 (m^{-1})*
0.37	13.36	2.22	0.48	10.60	1.64	0.48	9.73	1.17	0.4	10.02	2.03	0.43	9.73	1.57
0.9	11.11	1.86	1.03	11.52	1.74	1	9.44	1.51	0.97	12.15	2.38	0.95	11.23	1.97
1.91	9.79	1.53	2.04	11.92	2.15	2.01	7.26	1.40	2	10.94	1.74	1.95	11.80	2.20
2.94	11.80	1.80	3.04	10.77	1.86	3.03	11.29	1.34	3.01	15.83	2.84	3.01	9.56	1.80
3.95	10.42	1.97	4.06	9.33	1.57	4.05	11.63	1.34	4.06	11.75	1.40	3.99	10.94	2.03
4.95	10.88	1.80	5.05	25.33	3.76	5.07	10.60	1.34	5.12	9.16	1.80	5.00	7.95	1.86

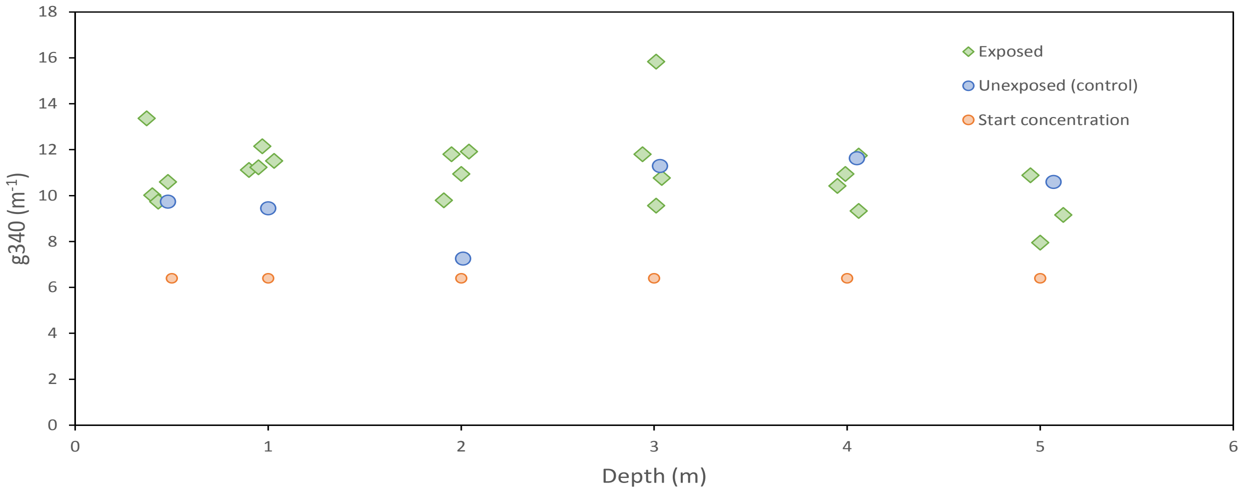

Figure 31: Graphical overview of the bleaching experiment absorbance data for each depth.

To test for a relation between g340 absorbance and depth of the bottle, a one-way ANOVA test was applied. This indicated that there was no significant difference between means of the different depths ($p = 0.473 > 0.05$). The mean of the exposed bottles and the mean of the unexposed bottles have also been analysed by the use of a one-way ANOVA test. This test showed that there was no significant difference between the means of the exposed and unexposed bottles ($p = 0.185 > 0.05$). Furthermore, the mean of the exposed bottles of the same depth have been compared to the unexposed bottle of that associated depth, using a one-sample t-test. Exposed bottles at depths of 1 and 2 m seem to have a significantly different g340 values than the unexposed bottle (respectively; $p = 0.003 < 0.05$, $p = 0.004 < 0.05$). However, this was not the case for remaining depths.

As it seems that no bleaching occurs at a depth of 0.5 meters and below, it can be concluded that most of the epilimnion is too dark for bleaching. Therefore the process of bleaching is of little account in the CDOM balance.

3.2.6 Stratification and CDOM concentration

Figure 32 shows the absorbance, g340, in the epilimnion and in the hypolimnion for each month. The hypolimnion has small fluctuations in absorbance with an average g340 value of 5.37 (m^{-1}) over the four months. The epilimnion has on average 11.7% higher levels of absorption. Absorbance levels in the epilimnion seem rather constant in the first three months, however in March the epilimnion absorbance decreases and reaches similar levels as the hypolimnion. In February the epilimnion contained 0.18 mg L^{-1} POC and 1.03 mg L^{-1} PON. The hypolimnion contained 0.01 mg L^{-1} POC and 0.11 mg L^{-1} PON, resulting in, respectively, a 94 and 89 % difference.

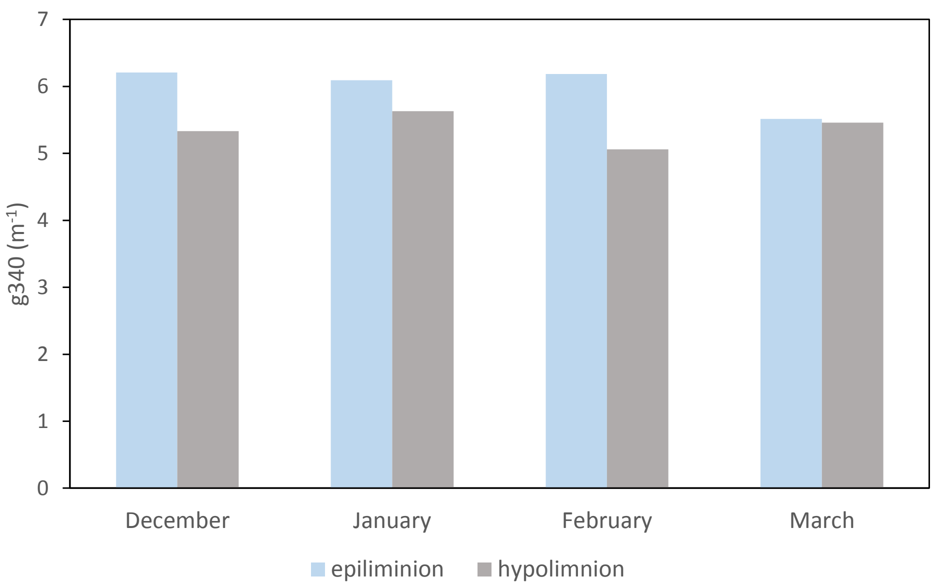

Figure 32: g340 absorbance in epilimnion and hypolimnion per month over the period of the thesis. Epilimnion samples are taken with a 25 meter tube. Hypolimnion sample depths are fluctuating; December 95 m, January 40 m, February and March 70m.

3.2.7 Summer CDOM balance

Data described in the previous sections were used to compute the CDOM balance (Table 7). It shows that during the summer more CDOM (23%) flowed into the lake then left the lake. Table 8 displays the relative CDOM inflow for each tributary per month. The crooked has the highest input in the first two months, and for the last two months the rest inflow has the highest input. Table 9 shows the relative importance of CDOM inflow per relative flow (Relative CDOM inflow divided by relative flow). The Hohonu has the highest CDOM inflow per flow. Figure 33 shows a comparison of g340 absorbance in the lake, with monthly average g340 absorbance in the inflow. Lake absorbance levels stay below inflow absorbance levels, indicating no net accumulation of CDOM in the lake.

Table 5: CDOM balance for each summer month

	g340 Inflow (m^2 month^{-1})					**g340 Outflow**	**CDOM Excess (m^2 month^{-1})**	
	Crooked	*Hohonu*	*Orangipuku*	*Rest*	**Total**	**Arnold**	Excess inflow	% of inflow
December	*8.19E+8*	*3.20E+8*	*4.24E+08*	*4.49E+08*	**2.01E+9**	**1.48E+9**	5.36E+8	26.6
January	*4.96E+8*	*1.58E+8*	*1.17E+08*	*2.08E+08*	**9.78E+8**	**8.44E+8**	1.35E+8	13.8
February	*2.18E+8*	*8.07E+7*	*5.06E+07*	*3.01E+08*	**6.51E+8**	**6.28E+8**	2.31E+7	3.5
March	*3.70E+8*	*1.96E+8*	*1.77E+08*	*5.50E+08*	**1.29E+9**	**8.52E+8**	4.41E+8	*34.1*
Overall	*1.90E+9*	*7.54E+8*	*7.68E+08*	*1.51E+09*	**4.93E+9**	**3.80E+9**	1.13E+9	23.0

Table 6: relative CDOM inflow of total per tributary per month.

	Relative CDOM inflow per tributary (%)				
	Crooked	Hohonu	Orangipuku	Rest	Total
December	40.7	15.9	21.1	22.3	100
January	50.7	16.1	11.9	21.2	100
February	33.5	12.4	7.8	46.3	100
March	28.6	15.1	13.7	42.6	100
Overall	38.4	14.9	13.6	33.1	100

Table 7: Relative CDOM input per relative flow for each tributary.

	Crooked	**Hohonu**	**Orangipuku**	**Rest**
relative CDOM input per relative flow (-)	0.79	1.96	1.06	1.07

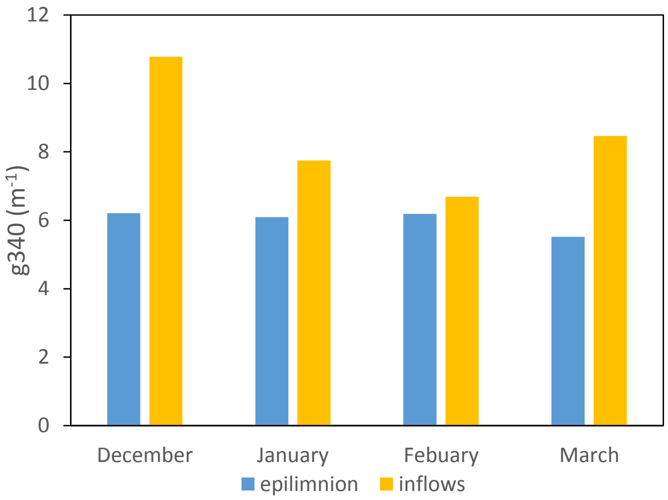

Figure 33: g340 absorbance in epilimnion compared to monthly average absorbance in inflows.

3.2.8 Longitudinal variation in CDOM

The next page gives a rough overview of sources of CDOM per tributary and increases in CDOM concentration from halfway to the ending of the river. Orangipuku and Crooked samples were taken on 10-3-2015 and Hohonu samples on 4-3-2015. Point eight of the Hohonu transect was calculated using the regression line in Figure 19, as no sample could be taken at the mouth at the time of sampling. The Crooked has a CDOM concentration about 5 times higher at the mouth than at bellhill bridge. The CDOM difference is about 1.8 times higher in the Hohonu between mouth and start of the transect.

Figure 34: Overview of Lake Brunner and its tributaries. g340 absorbance is given, sampled along the tributaries, at points of interest and at inflowing side streams (next page, 36)

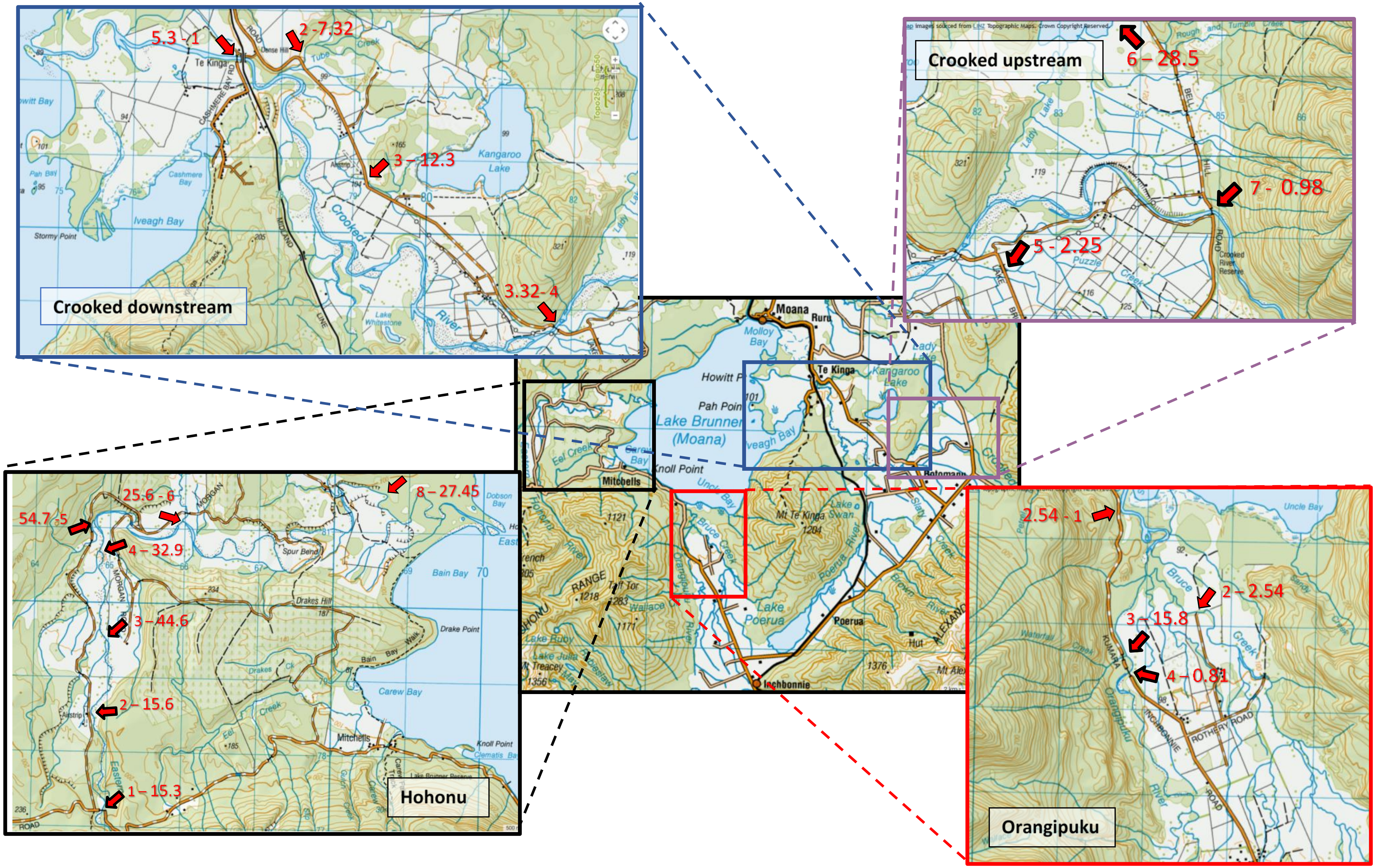

Crooked downstream
5.3 - 1
2 - 7.32
3 – 12.3
3.32 - 4
Crooked upstream
6 – 28.5
7 - 0.98
5 - 2.25
Hohonu
54.7 -5
25.6 - 6
8 – 27.45
4 – 32.9
3 – 44.6
2 – 15.6
1 – 15.3
Orangipuku
2.54 - 1
2 – 2.54
3 – 15.8
4 – 0.81
Lake Brunner
(Moana)

3.3 Results sub question 3: Reflection model

- Can an empirical model of reflectance be developed for lake Brunner? Reflectance is mainly dependent on the ratio of backscattering to absorption. Can a relatively low reflectance be linked with high CDOM concentrations and low chlorophyll *a* concentrations?

In figure 35, all values of R, and coefficients *a*, *b*, and *c*, computed with Kirks method, can be seen on a continuous time scale. It seems that the absorption coefficient is rather constant, and forms a base level of *c*. While the scattering coefficient mostly determines the fluctuation within the beam attenuation coefficient.

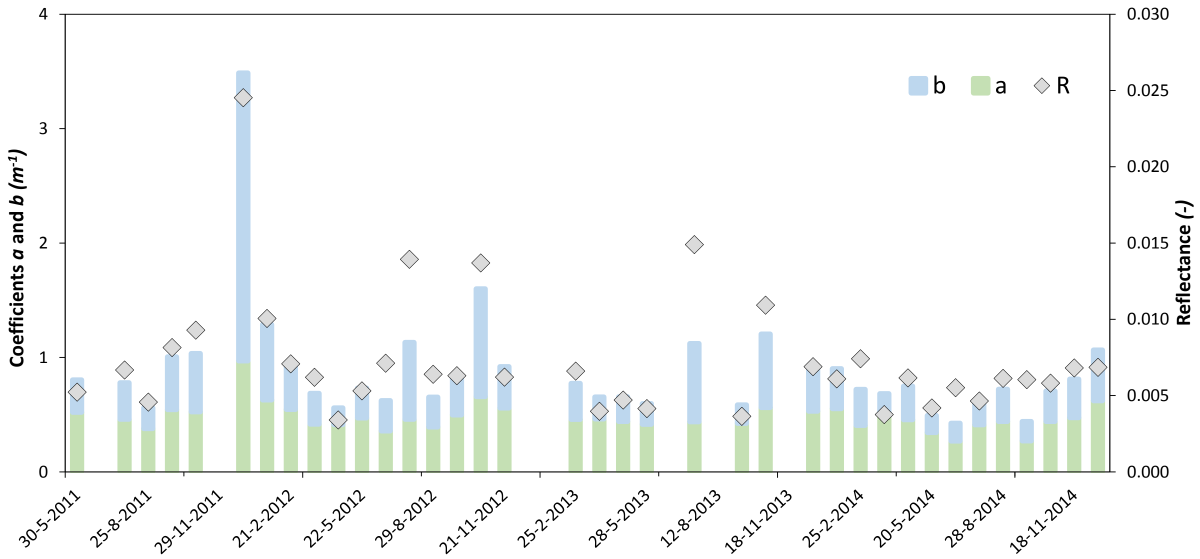

Figure 35: absorption (a) and scattering (b) coefficients, and reflectance shown over the period from May 2011 till December 2014. Beam attenuation coefficient is shown by both bars (a + b).

Figure 36 is an indication for the accuracy of the calculations by the Kirk method of coefficient *c*, and thus also of coefficients *a* and *b*. Values of *c* on the y-axis were calculated by equation (4) which uses black disk to estimate *c* (Davies-Colley and Smith 2001). The Kirk method calculated *c* mostly underestimates *c* estimated from black disk. However, this difference could be expected as Kirks method is based on a different water body. Furthermore, Kirks method predicts *a*, *b* and *c* for the whole PAR wavelength, while *c* from black disk only estimated *c* at a wavelength of 555 nm. As the underestimation is not large, it can be said that the calculations with Kirks method are accurate enough for further analysis.

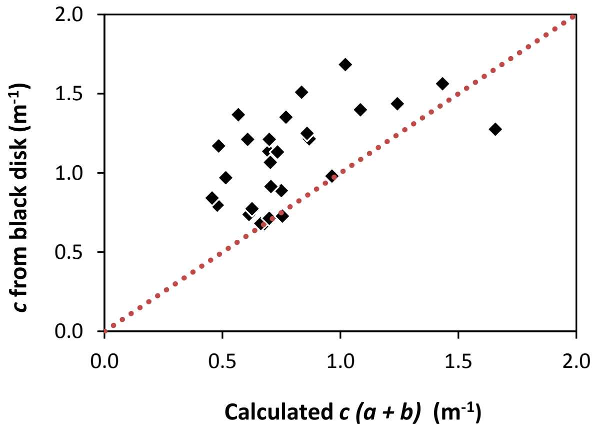

Figure 36: Beam attenuation coefficients c *calculated from black disk plotted against coefficient* c *calculated from* a *and* b.

The dependent variables R, *a*, *b* and, *c* have been analysed using multiple linear regression analyses with the water constituents as independent variables. However, independent variables are not allowed to be correlated to each other, as that would cause multicollinearity. Chlorophyll *a* and TSS, originating from data from May 2011 till December 2014, turned out to be correlated as is shown in Figure 26. The correlation was found significant ($p = 0.01$) with a Pearson correlation of $r = 0.385$. Chlorophyll most likely represents a part of the TSS during this period. This correlation was not found within data from the total dataset (1992-2014). The multiple linear regression analyses were therefore performed twice, with different variables, keeping the chlorophyll and TSS separated.

The results can be seen in Table 10 and Table 11. All independent variables were significant in the tests, apart from g340 in the correlation with R in table 10, which was only weakly significant.

Figure 16: Correlation between TSS and chlorophyll found in data from May 2011 till end of 2014. Overall dataset with data from 1992 till 2014 shows no significant correlation between these two variables.

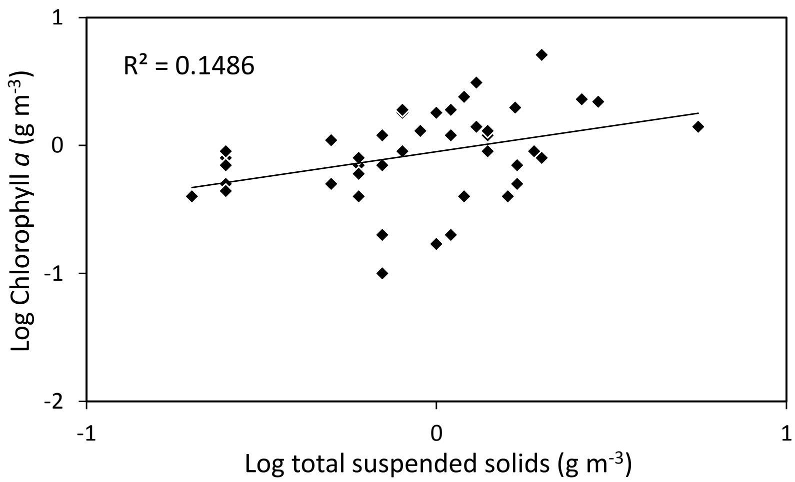

Table 8: Predictive models of R, and calculated coefficients a, b *and* c, *and significance of independent variables, chlorophyll and g340, computed by multiple linear regressions.*

			Log Chlorophyll *a*		**Log g340**	
	R^2	Intercept	p-value	slope	p-value	slope
Log R	0.158	-2.985	0.040	0.183	0.092	1.070
Log a	0.251	-0.824	0.008	0.126	0.048	0.658
Log b	0.251	-1.803	0.009	0.311	0.039	1.741
Log c	0.281	-1.022	0.007	0.208	0.023	1.233

Table 9: Predictive models of R, and calculated coefficients a, b *and* c, *and significance of independent variables, TSS and g340, computed by multiple linear regressions.*

			Log TSS		**log g340**	
	R^2	Intercept	p-value	slope	p-value	slope
Log R	0.284	-3.013	0.002	0.253	0.055	1.121
Log a	0.198	-0.879	0.028	0.100	0.033	0.730
Log b	0.326	-1.865	0.001	0.355	0.020	1.865
Log c	0.322	-1.086	0.002	0.219	0.012	1.325

4. Discussion

4.1 Discussion: Interactions with Brunner's light climate

The variables Secchi depth, chlorophyll *a* and total P were monitored on most sampling visits, and their datasets are most complete. However measurements for other variables, as black disk and CDOM, only started in recent years, and are at times inconsistent. Sampling visits have been inconsistent over time. Only since 2010 measurements were done on a scheduled, monthly basis. These data gaps effect the statistical analysis. Especially analyses concerning irradiance attenuation coefficients, black disk and g555, may lack a decent sample size, and might therefore not give robust results. Continuing current monitoring will reduce this uncertainty and might result in better predictive models.

Normal data distribution was necessary for most of the used statistical tests. However, due to gaps in the dataset, low sample sizes, or the nature of the variable (as for example chlorophyll), normal distribution was not achieved for all variables. Transformations were always performed to aim for a distribution closer to normal distribution. Again, increasing sample size may result in more normal distributed population in certain cases.

4.1.1 Visual clarity and light penetration

The results show that visual clarity in lake Brunner is significantly influenced by chlorophyll *a*. High chlorophyll *a* concentrations result in a lower visual clarity, and are thus inversely correlated. This is widely established by research, and one of the main negative effects of eutrophication (Vollenweider 1968). g340 and TSS were not significantly correlated with visual clarity, however the low p-value (0.08) of correlation of CDOM with Secchi is close to "significant" and might well have become so if the sample size were a little larger.

Equation 3 described in section 1.3 shows Secchi depth as a function of G, c and K (Preisendorfer 1986). Knowing that K is mainly dependent of CDOM (explained in detail below), and c consists of a part absorption *(a)* and scattering *(b)*, it would be reasonable to expect that CDOM, as main absorbent agent in lake Brunner, would affect Secchi depth. This would be in line with the model of Secchi depth, and further supports the concept of retaining CDOM in the (MLR) model.

Whereas chlorophyll had a significant effect on Secchi depth in Lake Brunner, it had no effect in Haupiri. The effect of chlorophyll is probably relatively negligible in Lake Haupiri as CDOM concentrations are about 5.5 times higher than Lake Brunner. Interesting is the significance of TSS in Lake Haupiri, while it has no effect in lake Brunner, with slightly lower concentrations.

Visual clarity measured by black disk is affected by chlorophyll and absorption by CDOM at 555 nm wavelength (g555). P-values for g340 and g440 show no significant results, but g555 is significant ($p = 0.035$), and thus indicates significance of absorption at this specific wavelength. This agrees with the finding by Davies-Colley (1988) of Eq. 4 in section 1.3, where Black disk is proportional to the beam attenuation coefficient, c_{555}, as has also been further explained in section 3.1 "Visual clarity – Black disk". However, as g555 is not the same as a_{555}, but rather a component, the formula cannot be used to calculate *a* or *b*.

Fee et al. (1996) researched effects on transparency (computed as; $T_{\%} = 100 * e^{-Kd}$), including effects of DOC and chlorophyll *a* in multiple Canadian Shield lakes. Both variables had an inverse effect on $T_{\%}$, but the DOC relationship was tighter than the chlorophyll *a* relationship. Using a specific attenuation coefficient (k_c = 0.016 m^2 mg Chl^{-1}) based on a study by Bannister (1974), the relative effect of chlorophyll *a* on K_d, and thus transparency, can be estimated (with $K_d = k_cC + k_w$). In the study of Fee et al. (median, range 1.6% - 30.9%) chlorophyll *a* was responsible for 6.6% of the variation of K_d. Combining these results it was concluded that DOC had the most effect on transparency. This partially agrees with the results of this research. K_d was significantly affected by CDOM, however not by chlorophyll. With a similar approach as Fee et al. chlorophyll is calculated to explain 2.6% (median, range 0.5% - 10.4%) of the variance in K_d. This value is low, and might therefore explain the statistical lack of influence by chlorophyll. However, we can conclude that CDOM is the main contributor to the irradiance attenuation coefficient. This is consistent with research on Australian dune lakes, in which CDOM was the main attenuator of $K_{d(PAR)}$, even though most of the monitored lakes were only slightly humic (range 0 - 27.8 m^{-1}, median 1.1 m^{-1}). In those lakes, both chlorophyll and TSS were not significantly related with $K_{d(par)}$ (Bowling 1988).

4.1.2 chlorophyll *a* and CDOM

Regarding the statistical results of the multiple regression analysis between CDOM and chlorophyll in lake Brunner, it seems that CDOM does not inhibit phytoplankton biomass in the mixed layer significantly. Likewise, the plot of average chlorophyll and phosphorus concentrations of New Zealand lakes seems to place Brunner on the regression line, and thus indicate little effect of competition for light for algal growth. Although, both other plots (figure 17 and 18) place Brunner below the regression, and thus indicate a lower Secchi depth than expected relative to chlorophyll and phosphorus concentrations. This might be explained by the negative effect CDOM has on Secchi depth, as discussed before. From these results it seems that CDOM does not inhibit algal growth in lake Brunner. However, these results do not necessarily take the compression of the photic zone into account. CDOM does effect K_d, as has been shown previously, and therefore reduces the euphotic depth ($4.6/K_d = z_{eu}$) (Kirk 2011). Calculated values of K_d vary between 0.54 and 0.79 m^{-1}. This results in euphotic depths of, respectively, 14.4 and 5.8 meter. Further calculations should be done to address how these changes in euphotic depth could affect algal biomass.

Calibrating the plots for amounts of CDOM in the lakes (e.g. colouring coding the humic concentrations of each lake within the plot) could show the possibility of inhibiting effects on phytoplankton growth in other lakes. Also, including more new Zealand lakes would optimize the regression as for example some quite humic stained West Coast lakes are currently not in the analysis.

Davies-Colley and Vant (1987) found only a weak positive relation between g440 and chlorophyll in 12 new Zealand lakes, when they hypothesized that more algae caused higher autochthonous CDOM concentrations. This corresponds with the finding of no inhibition of algal growth in Brunner. However, only three lakes had significantly high CDOM concentrations to cause substantial light attenuation, and most of the 12 lakes were eutrophic. A larger variety, and more lakes are needed to find our hypothesized negative relation.

A study by Jones (1992) discusses the theory of possible light competition between CDOM and chlorophyll. CDOM affects K_{par}, thus affecting available PAR throughout the water column, and therefore the euphotic depth, and thereby limiting the depth of phytoplankton growth. However, this potential effect can be reduced due to uneven distribution of algae throughout the water column. Motile and buoyant algae can change their position to maximize their photosynthetic ability, and evidence is available for flagellate algae being prominent in humic lakes. Insight in the Brunner's type and distribution of phytoplankton might thus give more clarification. Furthermore, Jones (1992) explains that mixing depth in summer is reduced due to stratification and therefore algae are more concentrated in the upper water column. Stratification thus decreases the time phytoplankton spend below the euphotic depth. This is true for Brunner with a mixing depth at around 10 meters during maximal stratification at the end of summer and an average euphotic depth of 8.7 m (2011-2014). Although the water column is only fully mixed during several winter months, partly mixing during other months already increases the time algae spent below the euphotic zone, as the lake is deep and the euphotic zone comparatively shallow. Thus this second argument does only decrease the limiting potential of CDOM during summer months. The most promising and logical explanation for the insignificance of the regression is that humic concentration is just not sufficient enough to markedly affect light attenuation. As Jones says that another study with maximum concentrations of 5 mg l^{-1} DOC is not enough to notice inhibiting effects. Lake Brunner's maximum DOC concentration over the total monitored period was only 3.9 mg L^{-1}. Haupiri's DOC concentrations were higher than 5 mg l^{-1} (7.6 –12.8 mg L^{-1}), and did show more clear effects of inhibition of algal growth.

The study of Carpenter et al. (1998) shows evidence for algal growth inhibition by CDOM. By being able to influence P-loading and CDOM concentration within the lake, interactions with chlorophyll *a* were studied over several concentration ranges. It was found that the mean and variability of chlorophyll *a* and primary production were decreased with increasing CDOM concentrations. The effect of increasing P-loading on chlorophyll *a* was supressed by a high CDOM concentration compared to a low CDOM concentration. Primary production rates (mg m^{-2} d^{-1}) could be decreased by 20% by increasing DOC concentrations by 4 mg L^{-1}. DOC concentrations in Brunner range only over 2.6 till 3.2 mg L^{-1}. An effect by these different concentrations might be too small for observation. Also, Carpenter et al. hypotheses that primary production might be maximised near or below DOC concentrations of 4 mg L^{-1}, by attenuating harmful UV radiation. If so, lake Brunner's CDOM would not inhibit algal growth, but rather facilitate more production.

Finally, Carpenter et al. (1998) concludes with the statement that if cultural eutrophication had not produced an enormous range of P input rates among lakes, limnologists would conclude that DOC and grazing were the most important factors controlling lake productivity. Interestingly, Francko (1986) arguments that inhibiting effects by humic matter are effects by chemical processes limiting micronutrients, e.g. iron, molybdenum, and thus not necessarily by light limitation.

4.1.3. Changes over time

The changes over time in Secchi depth and chlorophyll *a*, indicate a shift back to a more healthy lake system, towards its original state in 1992. Visual clarity, measured by Secchi disk and black disk, had a dip around 2004 till 2007, but have returned to similar yearly means in 2013 and 2014 as in 1992. Chlorophyll concentrations were low in 2013-2014, which seem comparable to 1992, and several significant higher peaks in between those years. However 1992-1993 do not have significant different means than the described peaks, and the peaks do not necessarily comply with the significant visual clarity changes. Interestingly, total P seems to fluctuate much over time, however has no significant different means. Although, 1992 and 2011 are nearly significantly different total P concentrations ($p = 0.07$). The peaks of chlorophyll and total P do not occur in the same years.

CDOM also shows differences in mean concentrations over time between 2004 and 2011, and an abrupt decline in 2012. Exact reasons can currently only be speculated. DOC concentrations in rivers and lakes in North America and northern Europe have been increasing during the past two decades. Monteith et al. (2007) demonstrates that DOC concentrations may have increased due to changes in deposition chemistry and catchment acid sensitivity. Atmospherically deposited anthropogenic sulphur and sea salt have declined, which increase the soil organic matter solubility through two mechanisms: By changing soil acidity and, or, by changing the ionic strength of the soil solution. However, this change in deposition is not necessarily a global phenomenon, and thus might not be relevant for New Zealand – in the much 'cleaner' atmosphere of the southern hemisphere. Gaiser et al. (2009) shows that changes in lake transparency can be linked to regional precipitation and resultant runoff of dissolved organic matter. Transparency was greatest in a lake in Florida during cool phases of the Atlantic Multidecadal Oscillation, which is associated with below-average rainfall. Transparency was lowest during warmer phases of this oscillation, which is associated with above-average rainfall. Therefore higher rain intensities will probably increase CDOM concentrations in lakes. Changes between 2004, 2011 and 2013 could thus be a result of different precipitation patterns.

The already wet West Coast region, where lake Brunner is situated, is predicted to become wetter still due to climate change. Annual precipitation levels for the area are expected to increase by 5% and 8% by 2040 and 2090, respectively, compared to 1990. Winter precipitation will increase by 11% and 21% by 2040 and 2090, respectively (Mullan and others 2008). Concentrations of CDOM will probably increase in lake Brunner over the coming decades, because of increasing precipitation (implying more leaching) and increased temperature (implying faster organic production).

4.1.4 Seasonality

Chlorophyll *a* concentrations are affected by the season. Winter has significant lower concentrations than other seasons. This can be explained by low productivity in the winter months of low light and low temperature compared to warmer seasons. No difference between autumn and summer months indicates no large reservoir of phosphorus in the hypolimnion, which is mixed into the epilimnion after destratification (Verburg 2009). Additionally, the lack of significant differences in total P between seasons indicate that seasonal differences in productivity are temperature-based, and affirms the lack of P renewal from deep water after destratification.

CDOM concentrations are significantly different between spring and summer. This can probably be explained by differences in CDOM inflow, stratification and increased productivity. As this also contributes to the CDOM budget, this will be discussed in more detail in section 4.2.5.

Lastly, reflectance has significant different means between autumn, and summer and spring. CDOM affects reflectance most strongly according to the MLR results, however seasonal changes do not agree between reflectance and CDOM. This significant difference in reflectance could be a result of small sample size. Increasing sample size is thus recommended.

As both chlorophyll *a* and CDOM attenuate light and are season dependent, visual clarity is also expected to fluctuate per season. However, visual clarity was found not significantly different between season. However, both Secchi disk and black disk seem to trend towards significance in terms of seasonal differences. Variability is high per season due to the changes over the measured years, which probably affects the statistical analysis. Enlarging the dataset might decrease the effect of the variability. Visual clarity would be expected lowest in the summer months. Interestingly, K_d is not affected by seasonality, while CDOM, its main influencing factor, does change with season. Seasonal fluctuations in CDOM are apparently small to change light attenuation.

4.2 Discussion: CDOM balance

There is much uncertainty and possible error regarding the CDOM balance. In each aspect of the balance there is some uncertainty. Below these uncertainties and other findings are discussed.

4.2.1 Rating curves

Firstly, the rating curves contain uncertainty regarding the higher flows of the Crooked and Hohonu. The last middle -to-high flow measurement of the Crooked seemed to deviate from the previous flow measurements. A shift in the bed may have occurred over the two months between the measurements, and influenced the flow dynamics. High Crooked flows might be underestimated by this rating curve. Furthermore, the Hohonu only has flow rating measurements up to average flow velocities. High flows might therefore be overestimated. These rating errors may result in possible overestimation of CDOM inflow by the Hohonu, and underestimation for the Crooked.

4.2.2 CDOM versus flow

Secondly, there is uncertainty within the CDOM *versus* flow plots. The high flow data points have only been measured over one or two events in a short time period. CDOM concentrations for a specific flow might differ per month or season. However, only a summer budget is computed, thus these measurements are probably sufficient.

The graphs 28, 29 and 30 show some interesting results. There is, for example, a difference in the CDOM lag time after the flood peak of each river. All three rivers have almost instantaneous increases in CDOM concentration during a flood peak. However, the CDOM lag time seems to be different per river. The Hohonu takes the longest to recover from a flood event. This lagging of CDOM has implications on the CDOM balance, as similar flows on the rising versus the falling limb of events have different CDOM concentrations. The variance in the Hohonu CDOM *versus* flow plot is therefore higher than the Crooked plot, as it has a longer lag time.

Another interesting incidental result of this research is the possible difference between CDOM inflows after a long dry period, and inflows after initial wet circumstances. In graphs 26 and 27, the first event occurred after a dry period without any heavy rains for about a month, while the second event happened only a couple of days later, with a pre-moistened catchment. The first event has a relatively larger increase in CDOM for both Crooked (5.8x higher than start) and Orangipuku (10.1x higher than start) than the other second event (respectively, 2.1 and 7.7x higher), while flows in the second event were much higher. This suggests a strong 'flushing' effect with the first event flushing out much of the 'accessible' pool of CDOM from catchment soils, and a muted response to the subsequent event.

Smith et al. (1997) theorize that during a flood event, soil water high in CDOM, rather than ground water or rain water dominates discharge, whereas base flows consists mainly of groundwater. An explanation for higher CDOM after drought, could be the longer retention time of soil water, and therefore more possibility for extraction of CDOM from the soil.

Missing a rating curve and correct water levels for Orangipuku provides even more uncertainty for the CDOM balance. Average daily flows and CDOM are very rough indicators, but are the only solution with the current data. The curve follows an exponential path, which might be realistic regarding the fast growing CDOM concentration at flood peaks and low CDOM levels at base flow.

4.2.3 Water balance

Uncertainty is also present in the lake water balance. The outflow and lake level change are continuously monitored and should thus be reliable. Precipitation and evaporation are values estimated from elsewhere in the region, and thus imprecise. Fortunately, the estimated values account only for about 5% of either these inflow or outflow.

While calculating the daily average flows of the Orangipuku, at times the calculated flow was larger than the leftover inflow (inflow – Hohonu + Crooked). At these times it was chosen to take only the leftover flow as Orangipuku flow. This shows the relative inflows of the tributaries fluctuate on a daily basis. Therefore again, inflows of the Orangipuku on daily basis might not be precise. However on the whole, calculated Organipuku inflows are only 1.2% less a contribution to the total inflow than estimated by Spigel and McKerchar (2008).

4.2.4 Photo bleaching

The bleaching experiment resulted in an unexpected outcome. No difference in CDOM between depths, and an increase, instead of decrease, of CDOM indicates no photochemical degradation of CDOM occurring at 0.4 meter and below. Unfortunately nothing can be said about possible bleaching rates above 0.4 meter, but it is hypothesized that this is the layer where bleaching should occur, as laboratory experiments have proven the degradation of CDOM by UV radiation (Bertilsson and others 1999; Bertilsson and Tranvik 2000; Dahlén and others 1996; Moran and Covert 2003; Salonen and Vähätalo 1994).

An in situ experiment by De Haan (1993) in the Tjeukemeer in the Netherlands concluded that humic substances are photodegraded at depths where UV radiation can penetrate. The daily degradation is similar to daily pelagic photosynthetic fixation of dissolved inorganic carbon in oligotrophic humic lakes. This experiment was conducted over several depths up till 25 cm, however clear bleaching only occurred above around 6 cm. However, Lake Brunner is much clearer than Lake Tjeukemeer.

Humic substances can function as a photochemical shield from UV-B radiation at concentrations of >4 mg/L, allowing the radiation only to penetrate several decimetres. Lake Brunner has a concentration of around 3 mg/L DOC, meaning that 1% of the surface UV- B radiation can penetrate to around 1.35 meters (Steinberg 2003).

In summer the epilimnion in lake Brunner ranges at 8 to 15 meters. Comparing this to the bleaching zone (lower than 2.5-5% of the epilimnion), it can be said that most of the epilimnion is ‘dark’ to photo bleaching and does thus not act as a significant sink of CDOM. Furthermore, residence time at the top layer of the epilimnion is short, as this layer is continuously mixed. CDOM is therefore only exposed for short periods to photo bleaching.

The results show an increase in CDOM in the tubes, which is on average 4.4 m^{-1} higher than the initial concentration. This is probably the consequence of degradation of POC. Therefore it is recommended to filter the lake water first for future bleaching studies, to reduce increases and noise in CDOM values. However, this is also an indication that CDOM itself increases within the lakes itself due to degradation of POC including phytoplankton. So, there is at least a small contribution to Brunner CDOM from autochtonous (in-lake) sources.

4.2.5 CDOM balance

Considering all the possible errors and uncertainties above we have now arrived at the combination of all the above together. New uncertainties also arise in the balance itself. The ‘rest’ inflow accounts for about a third of the CDOM inflow in to the lake with the current calculations and assuming, crucially, average concentrations of CDOM. However, the exact CDOM concentrations of all the small inflowing steams and runoff is unmonitored and thus unknown. The Carew stream accounts for 1.1% of the total inflow (Rutherford and others 2008). Measurements at high and low flow indicates that CDOM fluctuates enormously in the Carew (low; 4.1 m^{-1}, high; 43.1 m^{-1}). This ‘rest’ inflow originates from all along the lake, thus cannot be compared with the Carew alone. Therefore it has been chosen to take the average value of each tributaries’ average CDOM concentration (9.2 m^{-1}). This value is thus highly uncertain, and more research on this value would be needed.

Lastly, water levels were not logged on 69 days over the four months. CDOM inflow on these days has been calculated using the total inflow from the water balance and inflows for each tributary in percent. These inflows are thus estimations and differ from reality. Overall, it can thus be concluded that the balance has quite some uncertainties and is a rough estimation. Nevertheless it gives an indication of the fate of CDOM in the lake.

The CDOM balance indicates a higher inflow of CDOM (~20%) into the lake than is discharged, meaning that either accumulation of CDOM occurs in the lake or there are some unaccounted loss mechanisms within the lake. Accumulation does not seem to happen. Figure 32 shows monthly similar concentrations in eplimnetic CDOM, apart from a lower CDOM concentration in March, and thus no increase in concentration over time. The decrease in CDOM concentration in March seems counter logical, compared to the excess inflow of CDOM. Unfortunately, this data point cannot be revised due to the lack of additional eplimnetic CDOM samples in this month. Additionally, figure 33 shows no extra storage of CDOM in the lake either, as CDOM inflows are always higher than CDOM concentrations in the lake itself. Thus a sink of CDOM has to occur to account for the excess CDOM inflow.

Photo degradation in the upper most layer (<40 cm) could function as a larger loss mechanism than expected. As mentioned, the daily photo degradation is similar to daily pelagic photosynthetic fixation of dissolved inorganic carbon in oligotrophic humic lakes (Haan 1993), and thus masking bleaching effects. However, as daily pelagic production was not accounted for in the balance, bleaching cannot be the loss mechanism for the excess CDOM inflow.

A side result of the bleaching experiment indicated that POC was degraded into CDOM. Zhang et al. (2009) demonstrates CDOM formation from phytoplankton decay with a daily production rate of 0.08 m^{-1}. Although phytoplankton is much higher in the research of Zhang (2009), being research in a eutrophic lake, compared to Lake Brunner, it still affirms the possible contribution POC degradation to the CDOM balance. More importantly, increased terrestrial production in the catchment in summer would also be expected to yield more CDOM in the summer.

Figure 24 shows the tributary temperatures and a rough indication of epilimnion and hypoliminion temperatures throughout the sampling months. Tributary and lake surface temperature did change throughout these months, however hypolimnion temperature remained constant. As tributary temperatures were always higher than the hypolimnion, it can be expected that the hypolimnion is closed off for new inflows of CDOM. This could possibly explain the on average 10% difference between hypolimnetic and epilimnetic CDOM during the summer months. During summer months inflow is more stained by CDOM than inflows during winter months – due to greater CDOM production from catchment soils in summer. Stratification isolates less stained, winter water in the hypolimnion, while more stained summer inflows, supply the epilimnion with more CDOM. Interestingly, Figure 19 shows a similar concentration difference between spring and summer as the hypolimnion and epilimnion do, and this difference was significantly different. In addition, Davies-Colley and Vant (1987) found similar seasonality within humic lakes stained lakes, speculating the cause to be seasonal changes in precipitation. Both indicating winter inflows being less stained than summer inflows. As December is still early in the summer, it could be that the CDOM versus flow is different than measurements in March. Thus it might be that the inflows for December are an overestimation, explaining the large excess inflow in this month.

A research by McManus et al. (2003) suggests that CDOM is oxidised in the hypolimnion. Imbalances in calculations and measurements of deep lake oxygen and carbon suggests an additional sink of oxygen, caused by oxidation of CDOM. Accordingly, a decrease of ~15 µmol L^{-1} in dissolved oxygen was expected to have oxidised a DOC concentration of ~11 µmol L^{-1}. Between December and January a decrease of ~ 12 µmol $^{-1}$ dissolved oxygen occurred in lake Brunner's hypolimnion. Benthic oxygen consumption is unknown, however it can still be speculated that hypolimnion oxidation of CDOM may play a role in the CDOM balance. However hypolimnion CDOM concentrations seemed relatively constant throughout the summer months, and did thus not indicate any clear CDOM oxidation. The hypolimnion should be sampled more intensively to check for any clear changes.

Urban et al. (2005) studied DOC dynamics in lake Superior. A relation between chlorophyll and DOC had been found, indicating that fluctuations in DOC were due to productivity. Brunners' DOC is not correlated with chlorophyll due to its allochtonous nature, however it may be that seasonal differences in CDOM in the epilimnion are related to productivity. Urban et al. (2005) explains that 20% of DOC entering the lake is removed, which is interestingly the same as the excess CDOM inflow calculated in this budget. The removal mechanism was mainly allocated to bacterial respiration converting DOC into CO_2. Respiration was not found to be seasonally dependent. Bacterial respiration was calculated to be 1.1 - 13 times faster than photo chemical decay. This is conform with a more recent study by Koehler et al. (2014) who found that 10% of CO_2 emissions from lakes were photochemical-induced, and thus the major CO_2 release would be caused by bacterial respiration.

Another explanation as sink for CDOM could be sorption to particulate matter and deposition at the bottom. As CDOM is highly recalcitrant, it seems unlikely that all the excess CDOM is respired in this short period of time. Especially as hypolimnion CDOM does not change drastically throughout the summer months. Sorption could be another sink, however no further information is available for sorption in Lake Brunner.

As a last remark, the budget by Urban et al. contains more losses and gains than this budget describes. Shoreline erosion, precipitation, photosynthesis are additionally described as gains and respiration and sediment burial as losses. These factors have been partly discussed, but would make the balance much more complete if they were to be measured.

4.2.6 Longitudinal trends

The Hohonu river has the highest CDOM concentration, while the Crooked supplies the lake with the highest CDOM loading. The transects show that CDOM is mostly added during the lower reaches of the rivers. This can be explained by the steeper slopes and higher (colder) altitudes in the upper reaches of the rivers. The water flows faster through upland areas, limiting time to accumulate CDOM. Furthermore, the organic horizons in upland soils are thinner, and water is more fed by groundwater containing less organic matter than surface run off, and in any case, organic production (terminating in CDOM yield) is low due to cool temperatures. Thus CDOM is inversely related to slope, explaining also the higher CDOM in the less steep lower reaches (Rasmussen and others 1989; Seekell and others 2014). Furthermore, the wetlands in the region on the West Coast have soils low on aluminium and iron oxides due to extensive drainage of high annual precipitation. These oxides would otherwise immobilize humic substances (Gallegos and others 2008).

Another important factor is the vegetation in the catchment. While forest increases the amount of CDOM, cropland and grassland produces less CDOM. Furthermore, there is a difference in light attenuation attributes of CDOM depending on it source (Rae and others 2001). Moreover, CDOM originating from streams in human-modified areas are more recalcitrant to degradation. This results in initially higher concentrations in forest steams, which become eventually lower in concentration than in human modified streams, due to degradation of CDOM (Lu and others 2013).

The reason for the Crooked having less CDOM in the upper reaches than the Hohonu can thus be explained by steeper slopes and less vegetation (more area above treeline for the Crooked). For the lower reaches it can be seen that the catchment of the Hohonu is mostly forested, while the Orangipuku and Crooked lower catchments are more human modified, and thus have less forest and less CDOM. However all lower reaches supply more CDOM due to the lower slopes. Even though there are higher concentrations in the Hohonu, in the end, the Crooked delivers the most CDOM to the lake purely based on its large catchment area. Drainage ratio (catchment area / lake area) is positively related with CDOM loading (Rasmussen and others 1989; Seekell and others 2014).

Within the rivers these differences in CDOM concentrations can also be explained by the factors mentioned above. In the Hohonu for example, point 6 (Fig. 34) is a large inflowing stream, however contains less CDOM than was supplied before due to steep slopes in its origins. Interestingly, point 5 has the highest CDOM of all, while also originating from a more sloped area than for example points 3 and 4. Their catchments go mostly through grasslands, while point 5 completely lies in a forested area. It thus seems that vegetation is more important than slope in this case. Similar effects can be seen in the Crooked. For example point 2 has more CDOM due to its forested surroundings than point 5, while having similar slopes.

4.3 Discussion: Reflectance model

The model by Kirk, used to calculate *a*, *b,* and *c*, seems to be useful for estimations of the attenuation coefficients. In figure 36 it can be seen that values of *c,* calculated by black disk, are higher than calculated values of *c* by Kirks method. Kirks method thus seems to underestimate *c* values. However, considering that Kirks method was based on another water body, the values of $c_{black\ disk}$ and c_{Kirk} are still relatively close, and thus it is assumed that Kirks method is accurate enough for calculations regarding Lake Brunner.

TSS and chlorophyll *a* had been found correlated to each other (for the data of 2011 to 2014), as algal biomass is a part of TSS. R^2 values of regressions of R, a, b, and c, with TSS were all higher than these regressions with chlorophyll *a*. TSS seems thus a more accurate predictor for effects on R and the coefficients. Coefficient *c* had highest R^2 values, compared to *a* and *b.* This seems logical as c is the results of the combination of *a* and *b*.

Reflectance was low, as was expected for a dark lake as Lake Brunner. MLR models for R showed a correlation with g340 and either TSS or Chlorophyll *a* (due to their dependency*)*. TSS ($p = 0.002$) and chlorophyll *a* ($p = 0.04$) were more important influencing factors of R than g340 (p = 0.09 or 0.055), which p values were slightly above the confidence level of 0.05. This could be an indication of changes in relatively low TSS and chlorophyll *a* (resulting in more or less scattering) being more important than changes in relatively high absorbance by g340.

Furthermore, *a, b* and *c,* were all significantly correlated to g340 and either TSS or chlorophyll *a.* Remarkably, g340 was significantly affecting *b*. This should not be true, as CDOM is colloidal and thus only scatters negligibly. Also, slopes by g340 predicting R and *b* were positive, which would be expected to be negative, as CDOM diminishes backscattering of photons by absorption.

A research by Gallegos et al. (2008) studied two contrasting extremes of reflectance in four lakes, of which one is Lake Brunner. Differences over those lakes in reflectance were over a wide range (200 fold). Indicating that low reflectance in lake Brunner is due to high humic content, while high reflectance in glacial lakes were due to high TSS. Furthermore, these authors also found that particulate backscattering was higher in the humic-stained lakes than expected. Particulate scattering spectral exponents (0.80 for Brunner) were high, indicating scattering by small particles. Very fine, possible colloidal particulate matter (presumably aggregated humics) may accompany and contribute to this backscattering. This might possibly explain the correlation of CDOM with *b.*

5. Conclusion and recommendations

Current trends in chlorophyll *a* and visual clarity indicate a restoration of the lake's health towards similar levels as in 1992. Whether this is due to changes in agricultural practices or other causes as for example variability in decadal climate oscillations is unknown. This trend is only seen in the last two years (2013-2014), thus does not immediately prove a shift to a healthy state. Monitoring should continue to see whether this trend is holding.

An increased P loading will result in increased phytoplankton growth, which is apparently not inhibited by the current CDOM concentrations. CDOM does affect the euphotic depth, however, not enough to inhibit algal production. Increases in CDOM could eventually inhibit phytoplankton growth. However, fluctuations in CDOM on a seasonal scale and over the past decade proved to be low, thus needed increases for inhibition will probably not be achieved. Climate change will probably increase CDOM due to increased productivity (at higher temperatures) combined with increased precipitation. Currently CDOM might actually facilitate more phytoplankton growth by acting as a shield against biocidal solar UV-radiation.

CDOM inflows and outflows are not in balance in Lake Brunner over the summer months. Accumulation of CDOM in the lake is present in the summer, however not enough to account for the total excess CDOM inflow. As photo bleaching seems to be too low to account for the excess CDOM inflow, we must seek for other sinks of CDOM.

The method by Kirk can be used to estimate the attenuation, absorption and scattering coefficients. However, the estimated coefficients *a* and *b* give no immediate clear insight in the constituents of Lake Brunner's water. Statistical analysis of the coefficients does not clearly show the hypothesized concept where CDOM mostly effects the absorption coefficient and chlorophyll (or TSS) mostly effects the scattering coefficient.

Recommendations

- Current monitoring practices should be continued to track future trends. Furthermore, the extra data will reinforce the current statistical findings and providing more robust conclusions.
- Continue monitoring light penetration (K) and reflectance (R), so as to provide a dataset for further analysing optical character of Brunner.
- Calculations of the compression of the euphotic zone by CDOM would further check for any inhibiting effects on algal biomass, currently unaddressed in this study.
- Continue monitoring CDOM in at least one tributary (Crooked?) year round to test the hypothesis of seasonality explaining the lower hypolimentic versus epilimnetic CDOM.
- Year round sampling of hypolimnetic CDOM at same depth and additionally seasonal CDOM profiles would clarify changes in CDOM concentrations throughout the water column.
- To increase accuracy of CDOM balance, some ungauged inflows should be monitored to get more insight in actual CDOM inflows.
- More CDOM data in NZ lakes would be of interest to see if CDOM is the explaining factor for deviations in graphs 16, 17 and 18.

6. References

Abtew W, Melessa A. 2013. Chapter 8: Lake evaporation. Evaporation and evapotranspiration : Measurements and estimations. Springer. p. 109 -132.

Bannister TT. 1974. Production equations in terms of chlorophyll concentration, quantum yield, and upper limit to production. Limnology and oceanography 19(1):1-12.

Bastviken D, Persson L, Odham G, Tranvik L. 2004. Degradation of dissolved organic matter in oxic and anoxic lake water. Limnology and Oceanography 49(1):109-116.

Belzile C, Vincent WF, Howard-Williams C, Hawes I, James MR, Kumagai M, Roesler CS. 2004. Relationships between spectral optical properties and optically active substances in a clear oligotrophic lake. Water resources research 40:W12512.

Bertilsson S, stepanauskas R, Cuadros-Hansson R, Granéli W, Wikner J, Tranvik L. 1999. Photochemically induced changes in bioavailable carbon and nitrogen pools in a boreal watershed. Aquatic microbial ecology 19:47-56.

Bertilsson S, Tranvik LJ. 2000. Photochemical transformation of dissolved organic matter in lakes. Limnology and Oceanography 45(4):753-762.

Bowling LC. 1988. Optical Properties, Nutrients and Phytoplankton of Freshwater Coastal Dune Lakes in South-east Queensland. Australian Journal of Marine and Freshwater Research 39(6):805 - 815.

Carpenter SR, Cole JJ, Kitchell JF, Pace ML. 1998. Impact of dissolved organic carbon, phosphorus, and grazing on phytoplankton biomass and production in experimental lakes. Limnology and Oceanography 43(1):73-80.

Collier KJ. 1987. Spectrophometric determination of dissolved organic carbon in some South Island streams and rivers (note). New Zealand Journal of Marine and Freshwater Research 21(2):349-351.

Dahlén J, Bertilsson S, Pettersson C. 1996. Effects of UV-A irradiation on dissolved organic matter in humic surface waters. Environment International 22(5):501-506.

Davies-Colley RJ. 1978. Water appearance: Survey and interpretation. Water and soil miscellaneous publication. Wellington: Water & Soil Division, Ministry of Works & Development for the National Water & Soil Conservation Organisation. p. 66-78.

Davies-Colley RJ. 1988. Measuring water clarity with a black disk. Limnology and Oceanography 33(4):616-623.

Davies-Colley RJ, Ballantine DJ, Elliott SH, Swales A, Hughes AO, Gall MP. 2014. Light attenuation – a more effective basis for the management of fine suspended sediment than mass concentration? Water Science & Technology 69(9):1867-1874.

Davies-Colley RJ, Nagels JW. 2008. Predicting light penetration into river waters. Journal of Geophysical Research: Biogeosciences 113(G3):G03028.

Davies-Colley RJ, Smith DG. 2001. Turbidity, suspended sediment, and water clarity: A review. Journal of the american water resources association 37(5):1085-1101.

Davies-Colley RJ, Vant WN. 1987. Absorption of light by yellow substance in freshwater lakes. Limnology and Oceanography 32(2):416-425.

Davies-Colley RJ, Vant WN, Wilcock RJ. 1988. Lake water color: Comparison of direct observations with underwater spectral irridiance. JAWRA Journal of the American Water Resources Association 24(1):11-18.

Fee EJ, Hecky RE, Kasian SEM, Cruikshank DR. 1996. Effects of lake size, water clarity, and climatic variability on mixing depths in Canadian Shield lakes. Limnology and Oceanography 41(5):912-920.

Francko DA. 1986. Epilimnetic phosphorus cycling: Influences of humic materials and iron on coexisting major mechanisms. Canadian journal of fisheries and aquatic sciences 43(2):302-310.

Gaiser EE, Deyrup ND, Bachmann RW, Battoe LE, Swain HM. 2009. Multidecadal climate oscillations detected in a transparency record from a subtropical Florida lake. Limnology and Oceanography 54(6):2228-2232.

Gallegos CL, Davies-Colley RJ, Gall M. 2008. Optical closure in lakes with contrasting extremes of reflectance. Limnology and Oceanography 53(5):2021–2034.

Haan HD. 1993. Solar UV-light penetration and photodegradation of humic substances in peaty lake water. Limnology and Oceanography 38(5):1072-1076.

Jones RI. 1992. The influence of humic substances on lacustrine planktonic food chains. Hydrobiologia 229:73-91.

Kirk JTO. 1985. Effects of suspensoids (turbidity) on penetration of solar radiation in aquatic ecosystems. *Hydrobiologia* 28:195-208.

Kirk JTO. 1994. Estimation of the absorption and the scattering coefficients of natural waters by the use of underwater irradiance measurements. Applied optics 33(15):3276-3278.

Kirk JTO. 2011. Light and Photosynthesis in Aquatic ecosystems. Cambridge University Press.

Koehler B, Landelius T, Weyhenmeyer GA, Machida N, Tranvik LJ. 2014. Sunlight-induced carbon dioxide emissions from inland waters. global biogeochemical cycles 28:696–711.

Lu Y, Bauer JE, Canuel EA, Yamashita Y, Chambers RM, Jaffé R. 2013. Photochemical and microbial alteration of dissolved organic matter in temperate headwater streams associated with different land use. Journal of geophysical research: Biogeosciences 118:556-580.

McManus J, Heinen EA, Baehr MM. 2003. Hypolimnetic oxidation rates in Lake Superior: Role of dissolved organic material on the lake’s carbon budget. Limnology and oceanography 48(4):1624–1632.

Menken K, Brezonik PL, Bauer ME. 2005. Influence of Chlotophyll and Colored Dissolved Organic Matter (CDOM) on Lake Reflectance Spectra: Implications for measuring lake properties by remote sensing. Lake and reservoir management 22(3):179 - 190.

MfE. 1994. Water quality guidelines No. 2 : Guidelines for the management of water colour and clarity. Wellington: Ministry for the Environment.

Monteith DT, Stoddard JL, Evans CD, Wit HAd, Forsius M, Høgasen T, Wilander A, Skjelkvale BL, Jeffries DS, Vuorenmaa J et al. . 2007. Dissolved organic carbon trends resulting from changes in atmospheric deposition chemistry. Nature 450:537-540.

Moran MA, Covert JS. 2003. Photochemically mediated linkages between dissolved organic matter and bacterioplankton. Aquatic ecosystems: Interactivity of Dissolved Organic Matter. Elsevier science. p. 243-262.

Mullan B, Wratt D, Dean S, Hollis M, Allan S, Williams T, Kenny G. 2008. Climate Change Effects and Impacts Assessment. A Guidance Manual for Local Government in New Zealand. Ministry for the Environment.

Paerl HW, Payne GW, Mackenzie AL, Kellar PE, Downes MT. 1979. Limnology of nine Westland beech forest lakes. New Zealand Journal of Marine and Freshwater Research 13(1):47-57.

Preisendorfer RW. 1986. Secchi Disk Science: Visual Optics of Natural Waters. Limnology and Oceanography 31:909-926.

Rae R, Howard-Williams C, Hawes I, Schwarz A-M, Vincent WF. 2001. Penetration of solar ultraviolet radiation into New Zealand lakes: influence of dissolved organic carbon and catchment vegetation. Limnology 2:79-89.

Rasmussen JB, Godbout L, Schallenberg M. 1989. the humic content of lake water and its relationship to watershed and lake morphometry. Limnology and Oceanography 34(7):1336-1343.

Rutherford K, Chagué-Goff C, McKerchar A. 2008. Nutrient load estimates for Lake Brunner. Hamilton: NIWA.

Salonen K, Vähätalo A. 1994. Photochemical mineralisation of dissolved organic matter in lake Skjervatjern. Environment International 20(3):307-312.

Scheffer M, Carpenter S, Foley JA, Folke C, Walker B. 2001. Catastrophic shifts in ecosystems. Nature 413:591-596.

Seekell DA, Lapierre J-F, Pace ML, Gudasz C, Sobek S, Tranvik LJ. 2014. Regional-scale variation of dissolved organic carbon concentrations in Swedish lakes. Limnology and Oceanography 59(5):1612-1620.

Smith DG, Davies-Colley RJ, Knoef J, Slot GWJ. 1997. Optical characteristics of New Zealand rivers in relation to flow. Journal of the American Water Resources Association 33(2):301-312.

Spigel R, McKerchar A. 2008. Lake Brunner study: modelling thermal stratification. National Institute for Water & Atmosphere Research.

Steinberg CEW. 2003. Humic substances and global climate change. Ecology of humic substances in freshwaters. Springer. p. 117-130.

Urban NR, Auer mT, Green SA, Lu X, Apul DS, Powell KD, Bub L. 2005. Carbon cycling in Lake Superior. Journal of Geophysical research 110:C06S90.

Verburg P. 2009. Effects of nutrient loading in Lake Brunner. National Institute for Water and Atmosphere Research Ltd.

Verburg P. 2011. Disentangling effect of eutrophication and CDOM on visual clarity in Lake Brunner: preliminary data and methods. Hamilton: National Institute of Water and Atmosphere Research Ltd.

Verburg P, Horrox J, Chaney E, Rutherford JC, Quinn JM, Wilcock RJ, Howard-Williams CW. 2013a. Effects of nutrient loading on the trophic state of Lake Brunner. Marine and Freshwater Research 64:436–446.

Verburg P, Horrox J, Chaney E, Rutherford JC, Quinn JM, Wilcock RJ, Howard-Williams CW. 2013b. Nutrient ratios, differential retention, and the effect on nutrient limitation in a deep oligotrophic lake. Hydrobiologia 718:119–130.

Vollenweider RA. 1968. Scientific fundamentals of the eutrophication of lakes and flowing waters, with particular reference to nitrogen and phosphorus as factors in eutrophication. Paris: organisation for economic co-operation and development.

Xu CY, Singh VP. 2000. Evaluation and generalization of radiation-based methods for calculating evaporation. Hydrological processes 14:339 - 349.

Zaneveld JRV, Pegau WS. 2003. Robust underwater visibility parameter. Optics express 11(23):2997-3009.

Zhang Y, Dijk MAv, Liu M, Zhu G, Qin B. 2009. The contribution of phytoplankton degradation to chromophoric dissolved organic matter (CDOM) in eutrophic shallow lakes: Field and experimental evidence. Water Research 43:4685 - 4697.

7. Appendix

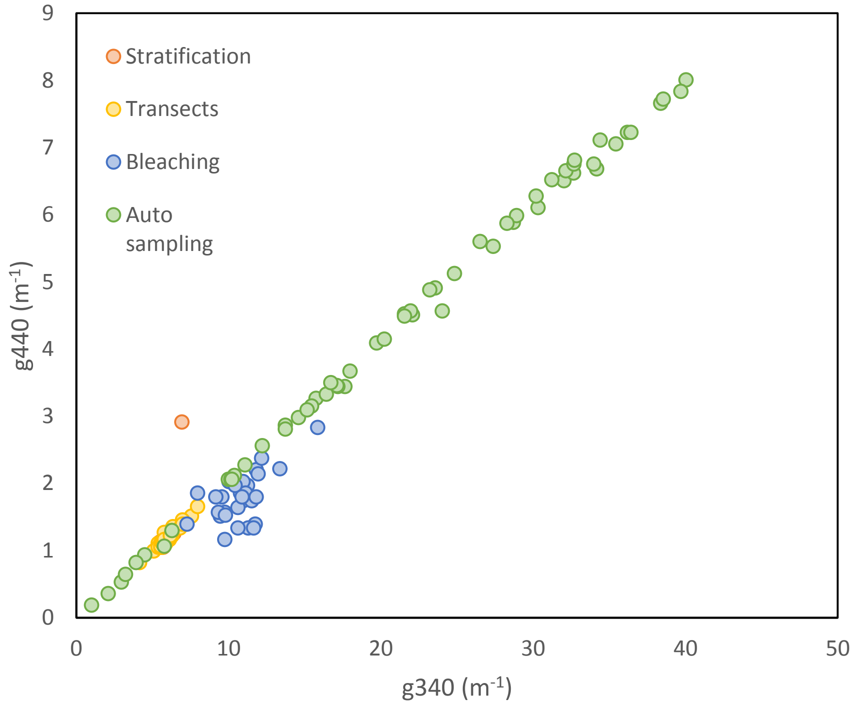

Figure 17: All g340 measurements plotted against g440 measurements. Measurements should roughly fall on the same line to be correct. As can be seen most bleaching experiment measurements and one stratification measurement are deviating from the regression line.